TABLE 1. SATELLITE OBSERVATIONS OF ALASKA AND KAMCHATKA VOLCANOES FOR THE MONTHS OF JANUARY-APRIL, 1997

January	**1**	**2**	**3**	**4**	**5**	**6**	**7**	**8**	**9**	**10**	**11**	**12**	**13**	**14**	**15**	**16**	**17**	**18**	**19**	**20**	**21**	**22**	**23**	**24**	**25**	**26**	**27**	**28**	**29**	**30**	**31**
Karymsky	X	X	X																												
Katmai	X	X	X																												

February	**1**	**2**	**3**	**4**	**5**	**6**	**7**	**8**	**9**	**10**	**11**	**12**	**13**	**14**	**15**	**16**	**17**	**18**	**19**	**20**	**21**	**22**	**23**	**24**	**25**	**26**	**27**	**28**
Karymsky	X	X	X	X	X	X	X	X	X																			
Mageik	P																											
Okmok	PX	X	X	PX	X	X	X	PX	PX	X	PX	PX	X	PX														

March	**1**	**2**	**3**	**4**	**5**	**6**	**7**	**8**	**9**	**10**	**11**	**12**	**13**	**14**	**15**	**16**	**17**	**18**	**19**	**20**	**21**	**22**	**23**	**24**	**25**	**26**	**27**	**28**	**29**	**30**	**31**
Amukta	**P**																														
Karymsky	X	X	X																												
Kliuchevskoi	X	X	X	X	X																										
Okmok	PX	X	X	X	X	X	X	PX	PX	X	PX	X	X	PX	PX	X	X	PX	PX	X	X	PX									

April	**1**	**2**	**3**	**4**	**5**	**6**	**7**	**8**	**9**	**10**	**11**	**12**	**13**	**14**	**15**	**16**	**17**	**18**	**19**	**20**	**21**	**22**	**23**	**24**	**25**	**26**	**27**	**28**	**29**	**30**
Klyuchevskoi	X																													
Okmok	X	P	X	X	X	X	X	PX	X	X	X	X	X	X	X															

Legend
X = Satellite observation of hot spots and/or plumes
P = Pilot Report

Seismicity

Although this is a double issue, for ease of comparison with other Bimonthly Reports discussion of the seismicity associated with the various volcanoes has been divided into the usual two-month intervals. Therefore, there will be two sets of the seismicity plots and histograms corresponding to the January/February and March/April intervals.

Akutan:

During January and February a total of 14 earthquakes were located in the vicinity of Akutan (figs. 5a, 14a and 15a). The largest event located during this time period had a magnitude of 2.2. The observed pattern of seismicity is similar to what has been observed in the past in the Akutan region. Two earthquakes were located near the head of Akutan Bay. Two events were located beneath the summit of Akutan and one event was located beneath the eastern flank of the summit. The remaining nine earthquakes, one of which was the magnitude 2.2 event, were located near the northwest coast of Akutan in the vicinity of Lava Point. These coastal events are of note in that they represent a small swarm of seismicity; all nine earthquakes occurred over a period of time of less than 24-hours. The observed rate of seismicity during this two-month period is nearly twice that of the previous two-month interval. It is, however, much lower than the six-month average of about 12 located events per month.

The March/April level of seismicity at Akutan continued at nearly the same rate as observed in January/February (figs. 5b, 14b and 15b). During March and April a total of 16 earthquakes were located in the vicinity of Akutan. The largest event located at Akutan had a magnitude of 2.1. This earthquake occurred northwest of the summit near the coast of Akutan Island at a depth of 6.5 km. During this two-month interval, eight additional earthquakes were also located in this region. Six earthquakes were located beneath the summit of Akutan. The one remaining earthquake was located about 3 km east of the summit. Seismicity has been observed in these three regions since the installation of the expanded Akutan seismic network in July 1996. Absent from the seismicity map (fig. 5b), however, is seismic activity in the general vicinity of the head of Akutan Bay. Activity in this region has been a persistent feature of the pattern of seismicity since seismic instruments were first deployed at Akutan during March 1996. Until now such activity was noted in every Bimonthly Report; at least one event was located in this region during each two-month reporting period. The first two-month interval lacking such seismicity, however, was actually February-March 1997. As noted above the observed rate of seismicity for March and April is only slightly higher than that of the previous two-month interval. Both observed rates are lower than the computed six-month mean seismicity rate.

Augustine:

There were 54 earthquakes located at Augustine during January and February (figs. 6a, 14a and 15a). The largest event located during this two-month period had a magnitude of 1.0. Many of these earthquakes appear to have been either related to the interaction of shore-ice and the coast or were related to cold weather in some other as yet not understood way. Such events generally occur only during periods of cold ($\leq -12^{o}$ C) weather and have distinctive waveforms. These waveforms are quite different from what is normally associated with Augustine events (see the previous Bimonthly Report for additional information regarding such events).

During this two-month interval a total of 36 earthquakes were located that do not appear to be weather related. The largest such event had a magnitude of 0.9. Of the 36 non-weather related earthquakes, 26 occurred during the month of February. Fifteen of these earthquakes occurred during a single day (February

continued

24, 1997). Note that this is the largest number of events to have been located at Augustine during a single day since AVO has had the capability to trigger on and locate small Augustine earthquakes. Furthermore, the monthly earthquake total for February is also the largest number of genuine Augustine events located by AVO during a single month. This seismic swarm has since died off and level of seismicity is once again at background level.

During March and April, nine earthquakes, the largest of which was had a magnitude of 0.6, were located in the vicinity of Augustine (figs. 6b, 14b and 15b). All of these events were located beneath the summit of Augustine at relatively shallow depth. The number of earthquakes located during this time period is much lower than that of the previous two-month interval as well as that predicted from the three-year mean seismicity rate. Note, however, that the apparent month-long period quiescence shown in Figure 6b may have, at least in part, been the result of station/telemetry problems experienced by several of the Augustine stations during that time.

Dutton:
Five earthquakes were located using data from the Dutton seismic subnet during January and February (figs. 7a, 14a and 15a). The largest of these events had a magnitude of 2.1. As can be seen in Figure 7a, four events were located approximately 25 km southeast of Dutton while the remaining earthquake was located 60 km to the southeast. Because of their distance from Dutton, all five earthquakes were probably regional tectonic earthquakes unrelated to volcanic activity at Dutton.

During March and April, seismic activity at Dutton appears to have been at background level (figs. 7b, 14b and 15b). Only one earthquake is plotted in Figure 7b. This event is nearly 80 km southeast of Dutton. Due to the considerable distance of this earthquake from Dutton, it is certainly a regional tectonic earthquake unrelated to volcanism at Dutton.

Iliamna:
During January and February a total of 163 earthquakes, the largest of which had a magnitude of 1.2, were located in the vicinity of Iliamna (figs. 8a, 14a and 15a). The number of located Iliamna events during this time period is considerably lower than that of the previous two-month interval. In fact, this represents a decrease in located events of 61% over a two-month period. Much of this decrease appears to have taken place after February 8, 1997 (fig. 8a).

The distribution of seismicity at Iliamna during this two-month interval defines three general regions of activity (fig. 8a). These clusters of seismicity are: a small group of earthquakes near the summit of Iliamna, a larger cluster of seismicity about 5 km south of the summit and a third somewhat smaller cluster of activity slightly east of the latter cluster. The first two regions of activity noted above have been present since this seismic swarm first started in August. The third grouping of events appears to have, at least in part, been present in the past; activity has previously been observed it the area defined by the western extent of this cluster. The present cluster, however, is more well defined and extends further east than it had in the past.

The most easterly of these events have probably been mislocated somewhat to the east due to an apparent change in station configuration resulting from station outages. During early January (January 3-7, 1997) the three components of IVE were operational only intermittently. They were, however, operational for a least a short time during each of the five affected days. Of the 13 most easterly events, 12 were located without the use of the IVE stations which implies that the station outage may have affected their locations. Further evidence of this comes from the earthquakes located during those periods in which the IVE stations were operational during this five day period. Weighting the IVE picks out and relocating such events often resulted in a significant eastward shift of epicenters to the general vicinity of the outlying earthquakes.

Note, however, that many of the earthquakes comprising this cluster of seismicity were located using the IVE stations. Therefore, the third cluster does appear to be a real feature of the seismicity pattern but it is probably not nearly as diffuse as shown in Figure 8a. In addition to the 12 potentially mislocated earthquakes discussed above, another 21 earthquakes were located without use of the IVE stations. Many of these events did not locate within the third cluster of seismicity. Since the IVE stations were operational intermittently during this 5-day period, some events were located using entire Iliamna network during this time. The locations of these events did not differ significantly from the 21 events discussed above, which implies that the locations of those 21 earthquakes are fairly reliable.

Activity at Iliamna continued to decrease during March and April (figs. 8b, 14b and 15b). Only 46 earthquakes, the largest of which had a magnitude of 2.0, were located in the vicinity of Iliamna during this two-month period. This represents about a 72% decrease in located earthquakes from that of the previous two-month period. The distribution of seismicity is similar to what it has been in the past. As has been the case since the onset of increased activity at Iliamna, clusters of seismicity are observed near the summit, however, and about 5-7 km south of the summit. The more easterly cluster south of the summit observed during the previous two-month interval is no longer present. This cluster of seismicity seems to have been replaced by a small grouping of earthquakes about 2 km south of the latter cluster, where seismicity has not been previously observed. Based upon the computed 22-month mean seismicity rate estimate the present level of seismicity at Iliamna is not yet at background levels, or at least it was not at the background level during this entire two-month period.

Katmai:
A total of 241 earthquakes were located in the Katmai/Valley of Ten Thousand Smokes region during January and February (figs. 9a, 14a and 15a). The largest such event had a magnitude of 1.9 and was located about 20 km east-northeast of Griggs.

As has been seen in the past, the seismicity is clustered into four general regions of activity. These regions of activity are a cluster near Martin/Mageik, a cluster near Trident, a cluster of activity northwest of Katmai Caldera, and a diffuse zone of seismicity east of Griggs. The observed rate of seismicity for this two-month period is lower than that for previous two-month interval as well as the 19-week mean value of about 130 located earthquakes per month.

During March and April, 269 earthquakes were located in the Katmai/Valley of Ten Thousand Smokes region (figs. 9b, 14b and 15b). The largest earthquake located during this time had a magnitude of 4.5. This event occurred on April 1, 1997 and was located about 5 km east of Trident. It generated over 50 aftershocks, the largest of which had a magnitude of 3.9, over the next five

days. The pattern of seismicity described above with respect to the January and February activity is also apparent in Figure 9b. The observed rate of seismicity for this two-month interval is greater than that of the previous two-month interval and slightly higher than the 260 located earthquakes predicted by the 19-week mean seismicity rate.

The observed seismicity rate for March and April is, however, probably an underestimation of the actual seismic activity in the region. Data from nearly half the Katmai seismic stations were lost at the end of April. On April 16, 1997, the failure of station KCG resulted in the loss of all the stations of the central Katmai seismic network (i.e. KGC, KEL, KVT, KBM, and KCE). This failure would not normally result in the loss of the other stations. A combination of problems resulted in the loss of the other four stations. Data from KCG as well as the other stations of central Katmai seismic network come into the receiver at KEL. During a station outage the receiver should squelch, thereby reducing the output from that station to zero. Unfortunately, for some reason, this was not the case with the KCG outage. Since the stations were not isolated via filter bridges, the noise from KCG (or what should have been KCG) was mixed with signals from the other four stations (Steve Estes and Guy Tytgat personal comm.). These stations were probably functioning well but the amplitude of the noise from KCG was such that their signals were essentially drowned out. The loss of five of the 11 Katmai stations is not blatantly obvious on the seismicity and histogram plots. This is, at least in part, due to a small swarm of activity that occurred on or about April 20, 1997 in the Martin/Mageik region. These earthquakes were sufficiently close to the remaining five fully operational stations (i.e. ACH, MGLS, KJL, CAHL, and CNTC) to allow them to be located. The final station, ANCK, was not functioning properly and would detect only the largest (M_L > 3) earthquakes so it was basically not a factor in earthquake detection and location. The loss of stations resulted in raising of the detection threshold from 0.0 to 1.2.

Makushin:
Four earthquakes, the largest of which had a magnitude of 2.3, were located in the vicinity of Makushin during January and February (figs. 10a, 14a and 15a). Three events, including the two largest Makushin earthquakes, were located in a tight cluster about 13 km southeast of the summit (~3 km from station MGOD). The remaining event was located about 5 km south of the summit. This is the first time seismicity has been observed in these two regions since monitoring Makushin began in July 1996. All four events were located in the 7-9 km depth range. The observed seismicity rate during this time period is a bit lower than the five earthquakes located in the previous two-month interval. Note that the six-month average for Makushin is about three located earthquakes per month.

A total of three earthquakes were located in the vicinity of Makushin during March and April (figs. 10b, 14b and 15b). The largest located event had a magnitude of 1.8. Two of the earthquakes were located about 8 km northeast of the summit near station MSW. Seismicity has not been previously observed in this region. The remaining event was located about 5 km south of the summit. As noted above, seismicity was first observed in this area during the previous two-month period. All three events had depths in the 2-5 km depth range, which is somewhat shallower than has usually been the case in the Makushin region. The observed rate of seismicity at Makushin during March and April is a bit lower than that of the previous two-month interval, and is nearly half the expected value based upon the six-month mean seismicity rate.

Pavlof:
During January and February, six earthquakes were located in the Pavlof region (figs. 11a, 14a and 15a). The largest of these events had a magnitude of 2.3. All six of these earthquakes occurred along the eastern flank of Pavlof Sister during a single day (i.e. January 10, 1997). This sequence is believed to be a small seismic swarm rather than an aftershock sequence because the largest earthquake occurred fairly late in the sequence and all the earthquakes are nearly the same magnitude (i.e. M_L 1.8-2.3). As one would expect, this earthquake swarm has skewed the observed rate of seismicity such that it is greater than that of both the previous two-month interval and the 6-month average (i.e. 2 located earthquakes per month).

It was very quiet at Pavlof during the months of March and April (figs. 14b and 51b). No earthquakes were located in the general vicinity of Pavlof during this two-month period. No events were even sufficiently large to meet the helicorder counting criteria (fig.14b).

Redoubt:
A total of nine earthquakes, the largest of which had a magnitude of 1.1, were located in the vicinity of Redoubt during the months of January and February (figs. 12a, 14a and 15a). Two earthquakes were located about 13-15 km northeast of the summit of Redoubt. Two events were located over 15 km to the northwest of the summit. In view of their relatively large distance from Redoubt, these four earthquake are probably regional tectonic events unrelated to volcanic activity at Redoubt. The remaining five earthquakes were located within a 10 km radius of the summit of Redoubt. Three earthquakes were located about 3 km southeast of the summit. The remaining two events were located beneath the northern flank of Redoubt about 5 km from the summit. Earthquakes are often located beneath the northern flank of Redoubt while events located to the southeast of the summit are less common but are by no means unheard of. The observed rate of seismicity during this time period is lower than that of the previous two-month interval as well as the three-year average.

During March and April, a total of 14 earthquakes were located in the vicinity of Redoubt (figs. 12b, 14b and 15b). The largest of such events had a magnitude of 1.2. One earthquake was located about 16 km east-northeast of the summit of Redoubt. Another earthquake was located about 17 km north of the summit. Because of their distance from Redoubt these two events are probably tectonic earthquakes that just happen to locate in the vicinity of Redoubt. Twelve of the 14 located earthquakes were located within a 10 km radius of the summit. Ten of these events were located beneath the northern flank of Redoubt. The other two proximal events were located about 3 km east and southeast of the summit. The distribution of seismicity at Redoubt during this two-month period is similar to what has been observed there in the past. The observed rate of seismicity is greater than that of the previous two-month interval but is somewhat lower than the three-year mean seismicity rate. This statement applies both to all the earthquakes plotted in Figure 12b as well as those event located within a 10 km radius of the summit of Redoubt.

continued

Spurr: During January and February, a total of 193 earthquakes were located in the general vicinity of Spurr (figs. 13a, 14a and 15a). The largest earthquake located during this time period had a magnitude of 2.5. The vast majority of these events were located in the Strandline Lake region (i.e. the northeast corner of fig. 13a) and represent a rather persistent swarm of regional tectonic earthquakes. There were, however, a total of 24 non-Strandline Lake events, the largest of which had a magnitude of 1.4, located during January and February. Ten of these earthquakes were located well to the south of Spurr and are probably regional events unrelated to activity at Spurr. The remaining 14 earthquakes were all located within 10 km of the summit of Spurr. Two such events were located about 6 km west-southwest of the summit. One event was located about 4 km south of the summit which is slightly north of Crater Peak. Another event was located about 6 or 7 km north of the summit. Based upon its relatively low frequency character, this event was designated as being a b-type event. The remaining 10 non-Strandline Lake earthquakes were located beneath the summit region of Spurr. Nine of these events form a general north-south trending zone of seismicity slightly east of the summit. Two such events were defined as being hybrid events based upon their waveforms. Hybrid earthquakes have unique waveforms in that they exhibit both a high frequency component characteristic of the usual volcano-tectonic earthquakes (i.e. a-type events) as well as a low frequency component which is characteristic of b-type events. The shallower of the two earthquakes was located 6 km west-southwest of the summit, and was also designated as being a hybrid event.

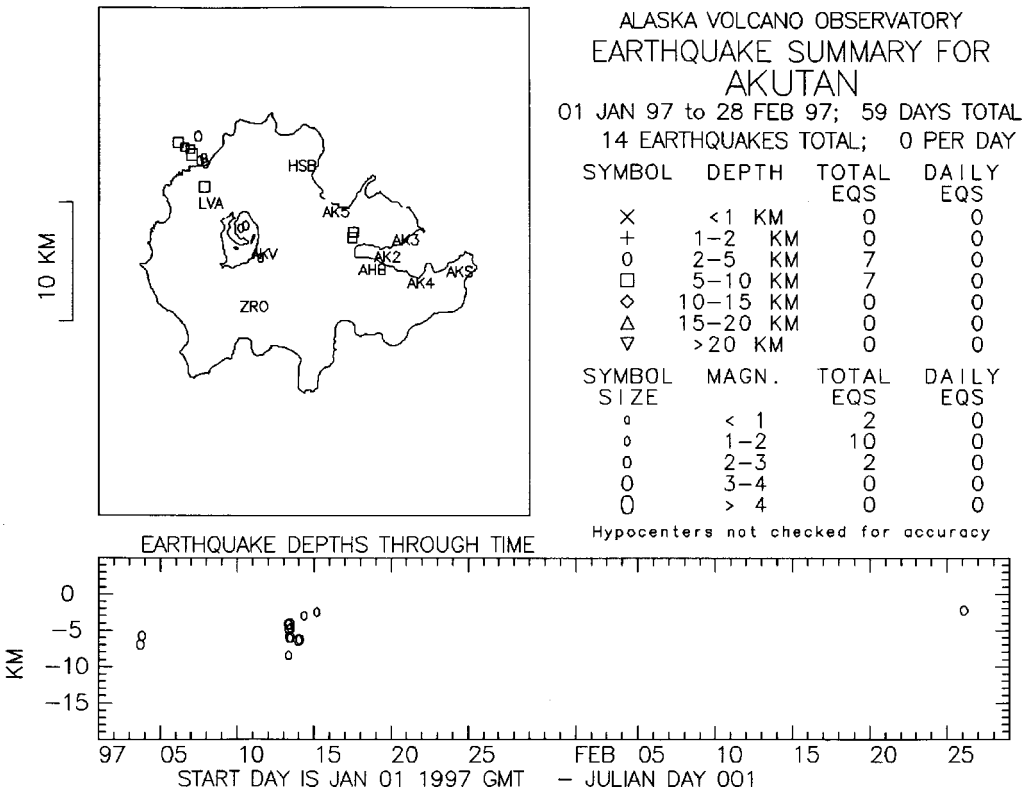

Figure 5a: Locatable Akutan seismic events in space and time for January through February.

The observed distribution of seismicity in the Spurr region during this time period is similar to what has been observed there in the past. During January and February the number of non-Strandline Lake events is a bit lower than that of the previous two-month period (i.e. 24 vs. 28). The same can also be said of those events having locations within a 10 km radius of the summit (i.e. 14 vs. 16). Note also that both sets of seismicity rates are lower than the corresponding three-year average seismicity rates.

A total of 181 earthquakes, the largest of which had a magnitude of 2.6, were located in the vicinity of Spurr during the months of March and April (figs. 13b, 14b and 15b). Most of these event were located in the Strandline Lake region, and as noted above they are probably regional tectonic events unrelated to activity at Spurr. Of the 181 located events, only 18 were not located in the Strandline Lake region. The largest of these non-Strandline Lake earthquakes had a magnitude of 0.6. Nine of these event were located well to the south of Spurr and are probably just regional tectonic earthquakes. The remaining nine events all locate within a 10 km radius of the summit of Spurr. Five such events were located beneath the summit of Spurr. One event was located about 9 km west of the summit. Based upon its waveform, this event was classified as being a hybrid event. One event was located about 4 km north of the summit. One event was located about 8 km northeast of the summit, and the final event was located about 5 km north-northeast of the summit. The waveform of the latter earthquake was such that it is classified as being a b-type event. The observed rate of seismicity within a 10 km radius of the summit of Spurr is less than half the value of the previous two-month period. This rate is also much lower than the three-year average rate of 9.4 located events per month.

Scott Stihler, Dan Wiesneth, Michelle Harbin, Cristyn Presley, John Benoit, Guy Tytgat, Pete Stelling, Michelle Coombs, Bob Hammond, Steve McNutt, and Art Jolly

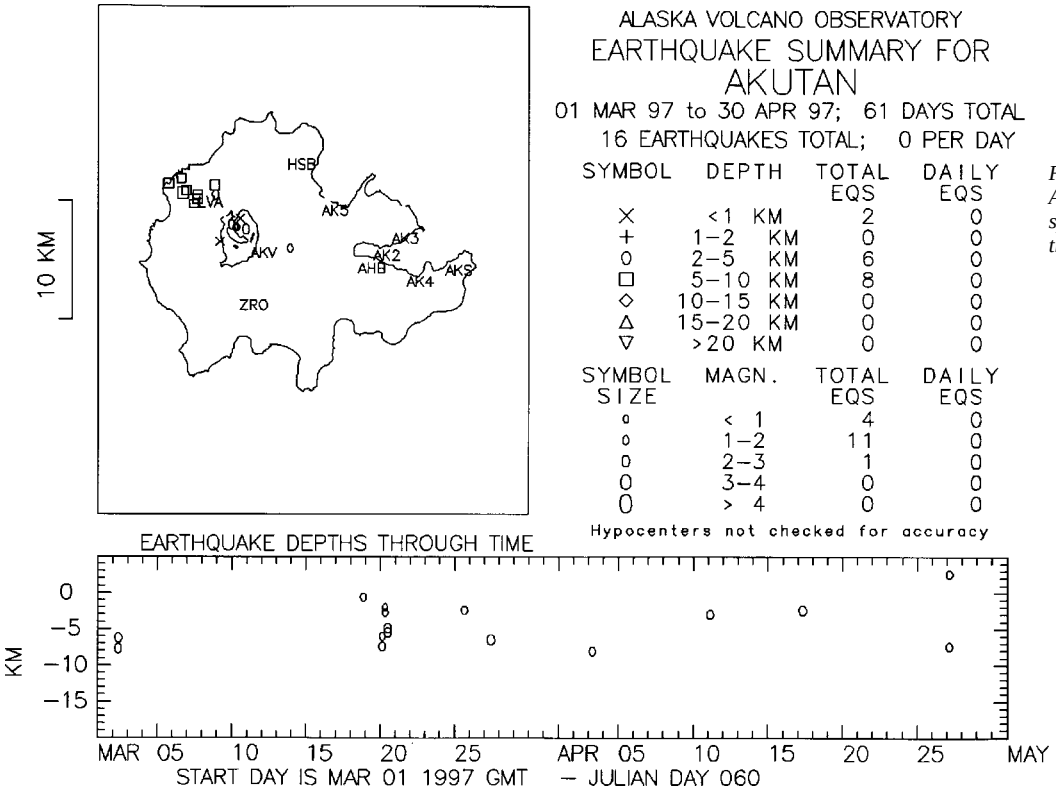

Figure 5b: Locatable Akutan seismic events in space and time for March through April.

Figure 6a: Locatable Augustine seismic events in space and time for January through February.

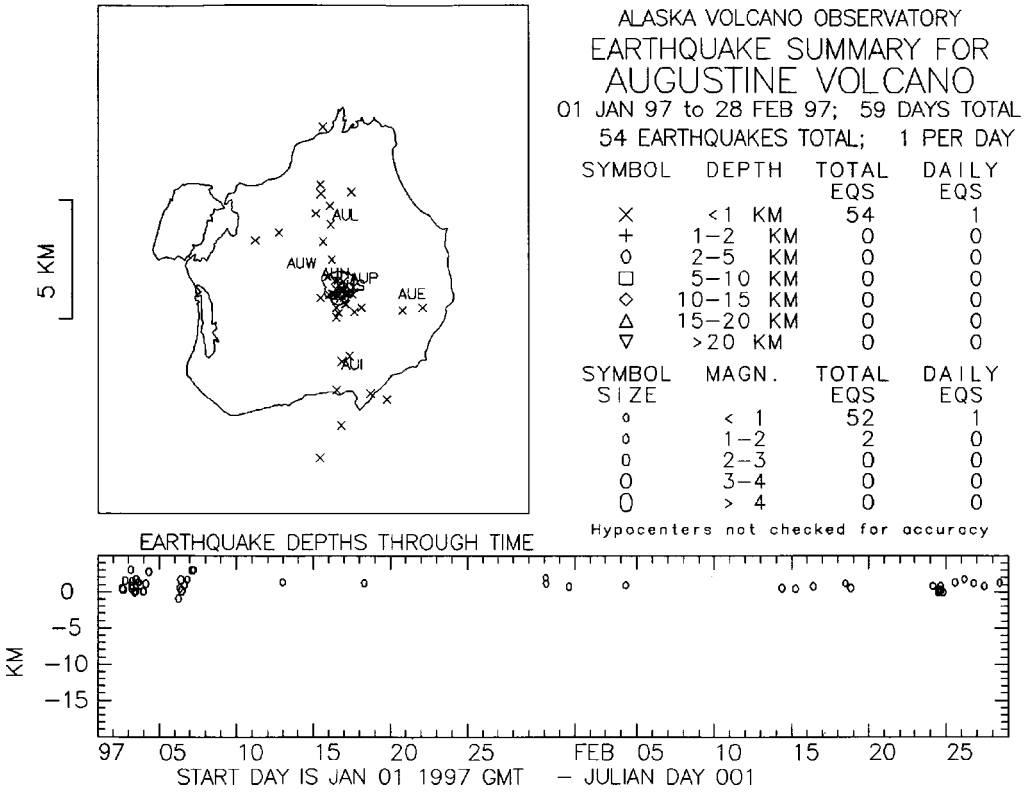

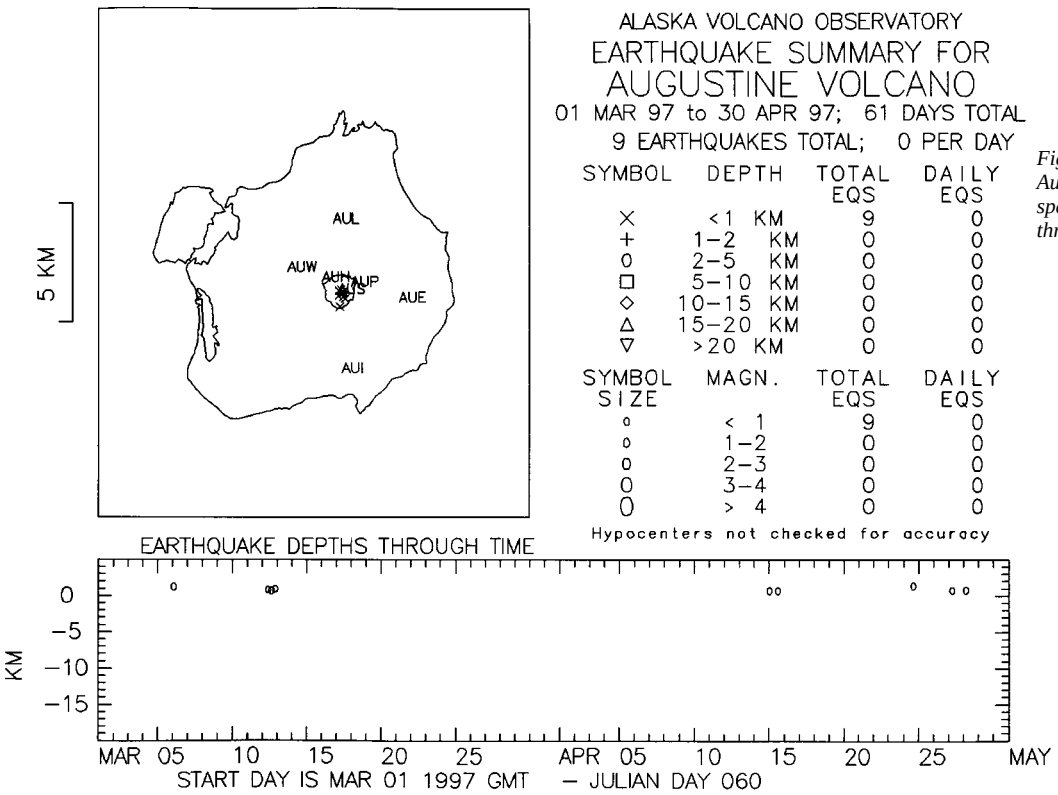

Figure 6b: Locatable Augustine seismic events in space and time for March through April.

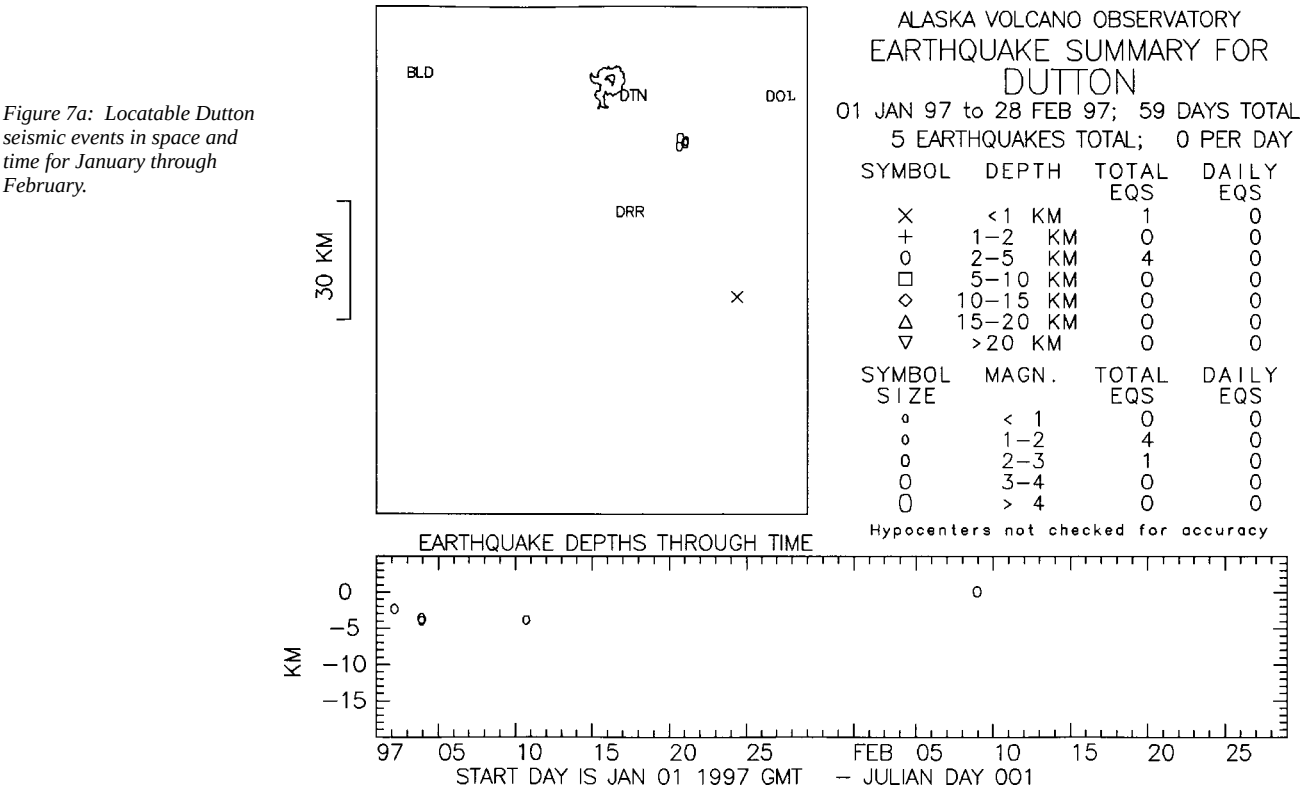

Figure 7a: Locatable Dutton seismic events in space and time for January through February.

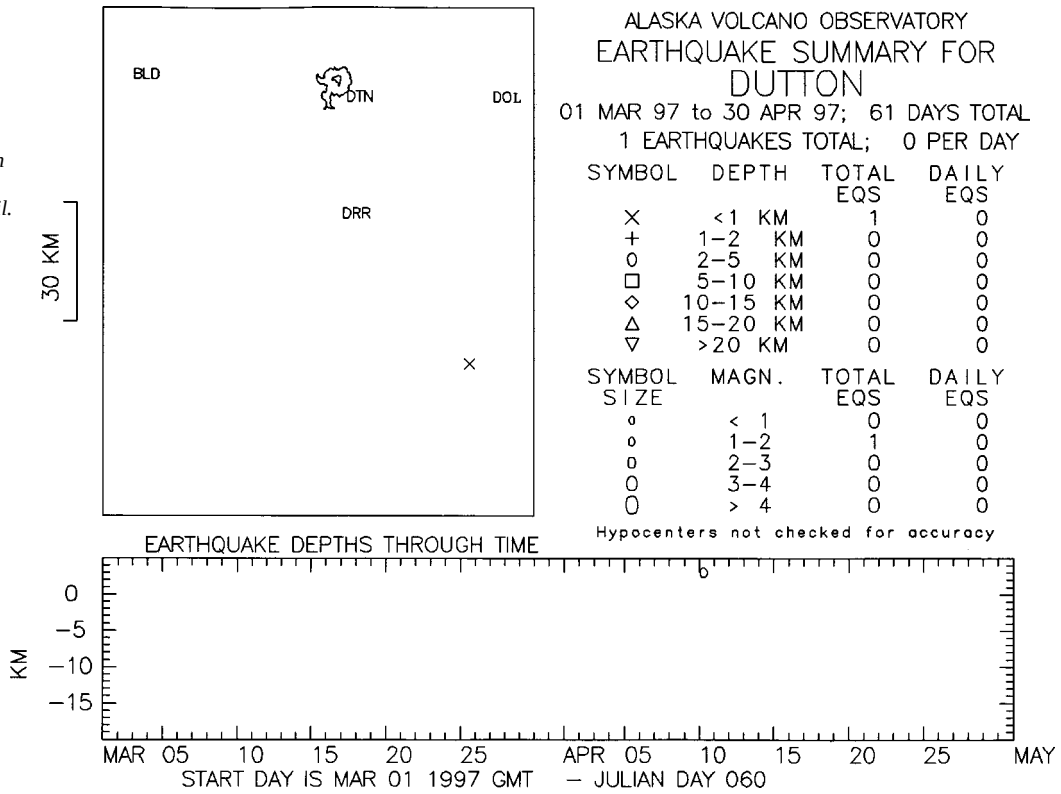

Figure 7b: Locatable Dutton seismic events in space and time for March through April.

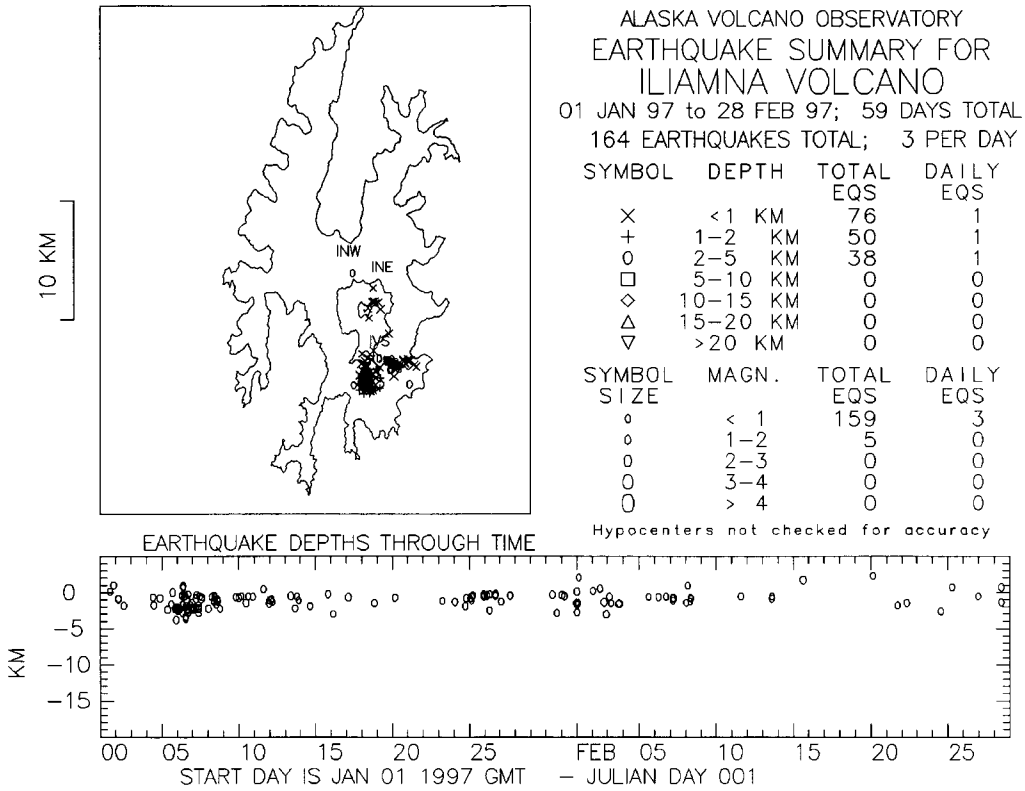

Figure 8a: Locatable Iliamna seismic events in space and time for January through February.

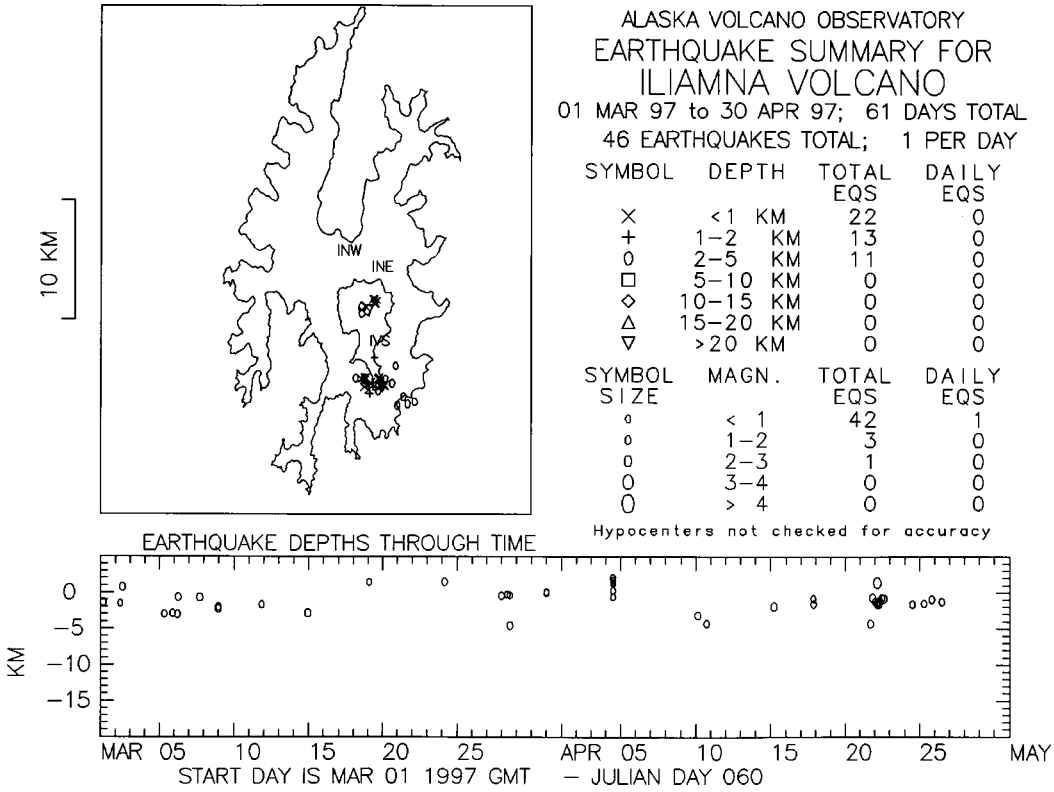

Figure 8b: Locatable Iliamna seismic events in space and time for March through April.

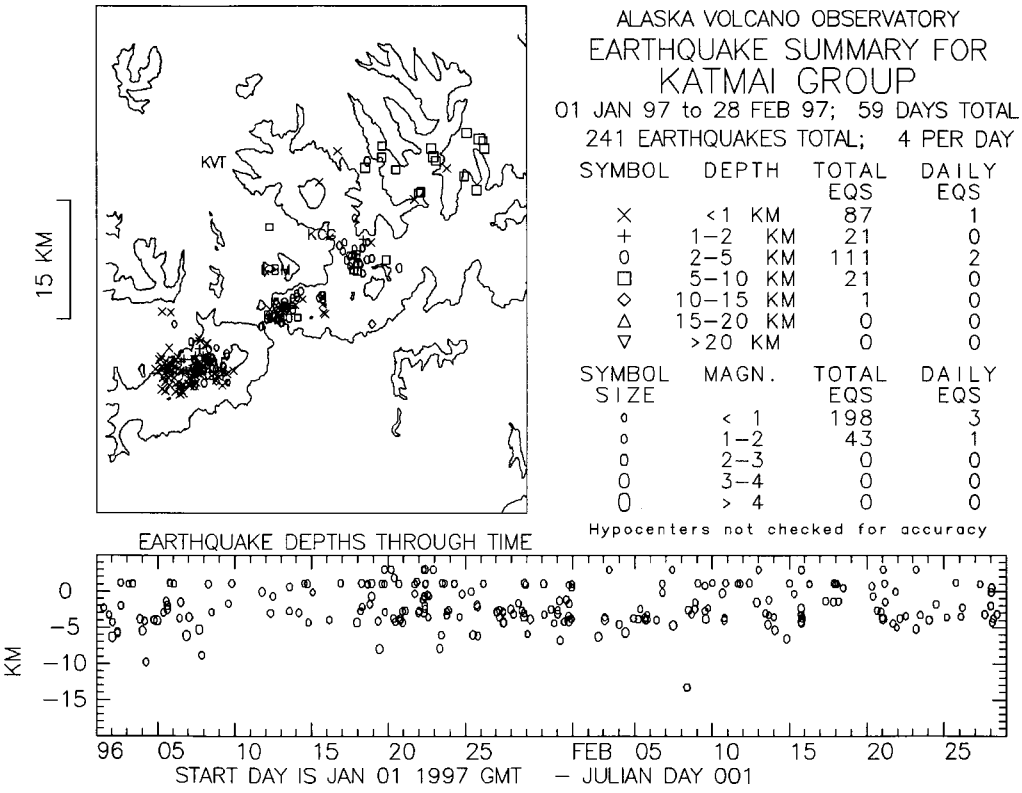

Figure 9a: Locatable Katmai seismic events in space and time for January through February.

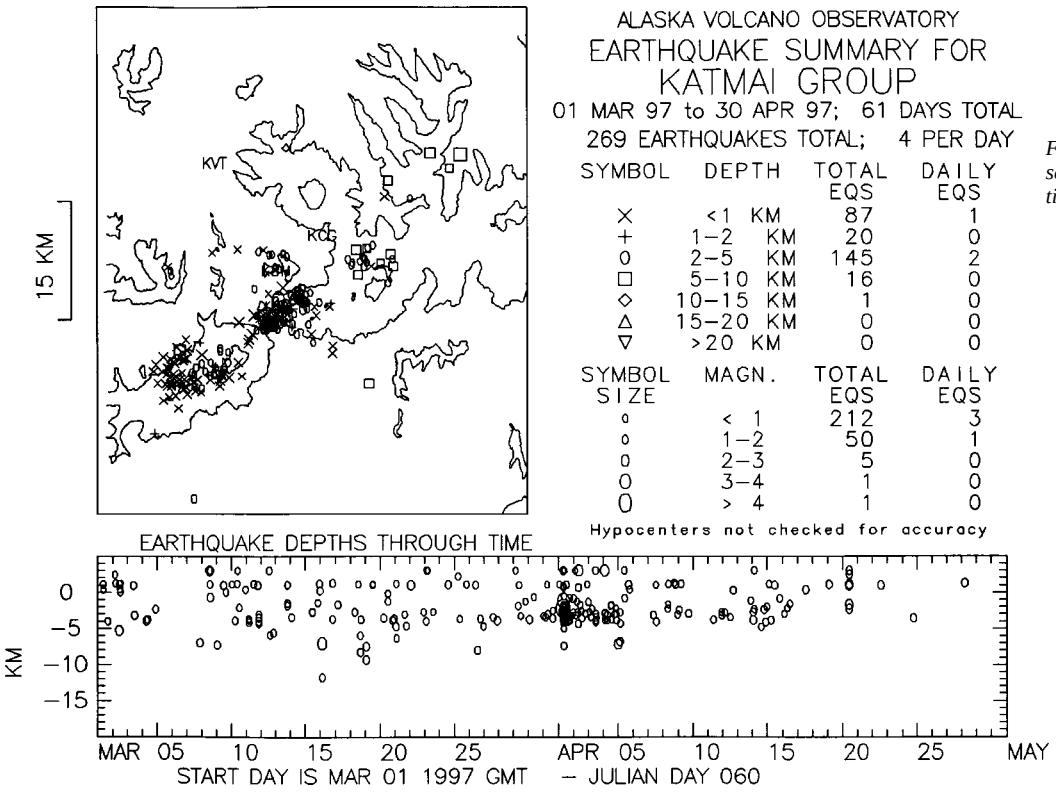

Figure 9b: Locatable Katmai seismic events in space and time for March through April.

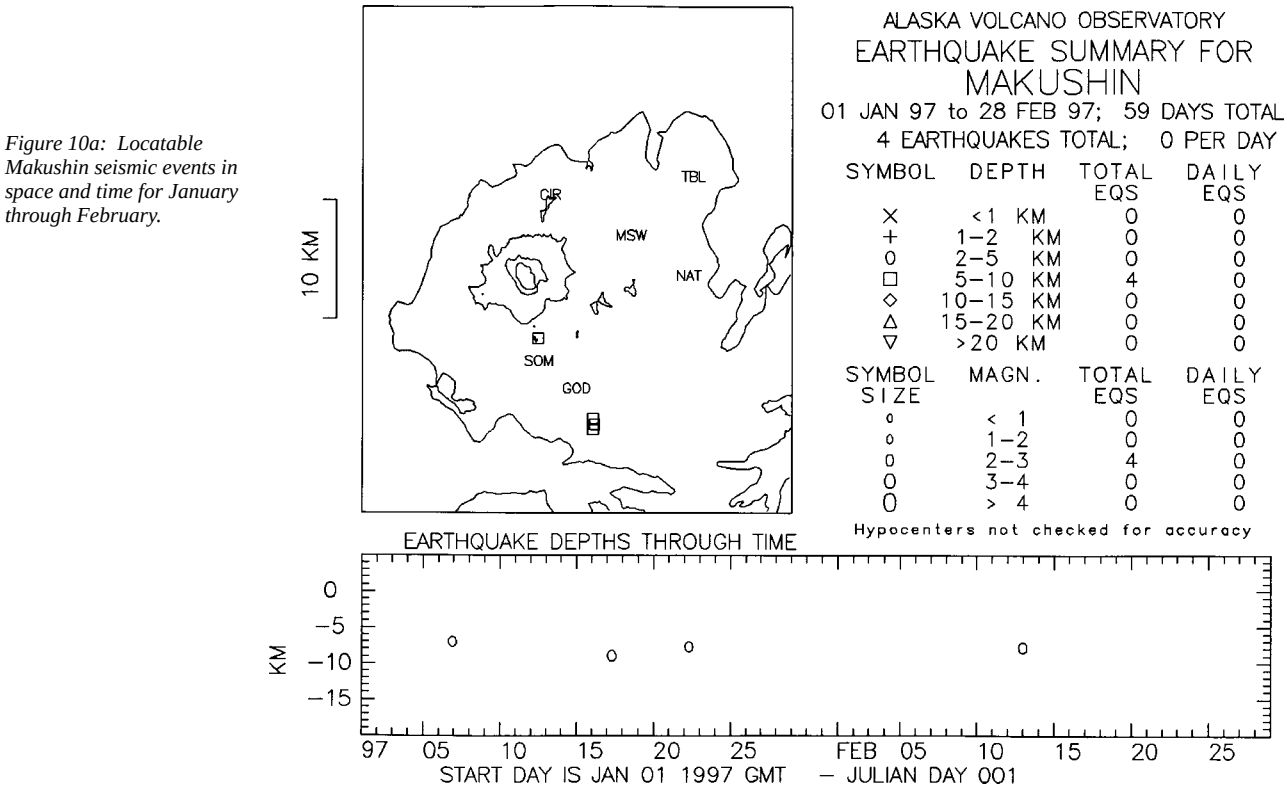

Figure 10a: Locatable Makushin seismic events in space and time for January through February.

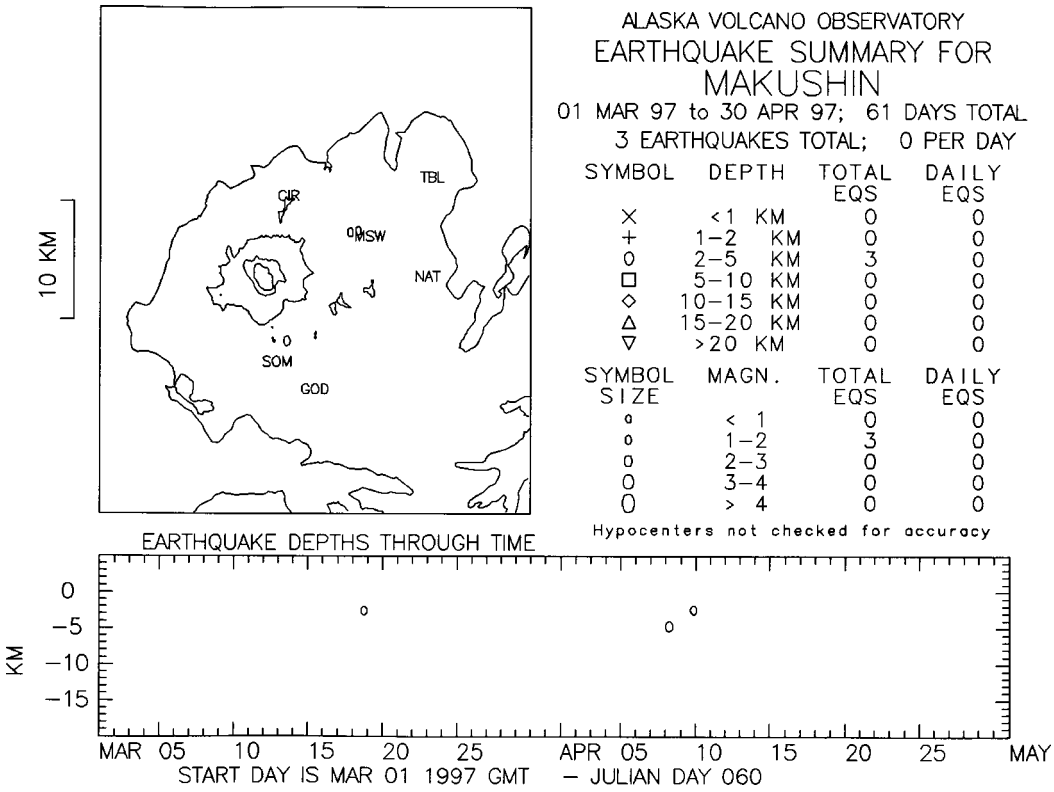

Figure 10b: Locatable Makushin seismic events in space and time for March through April.

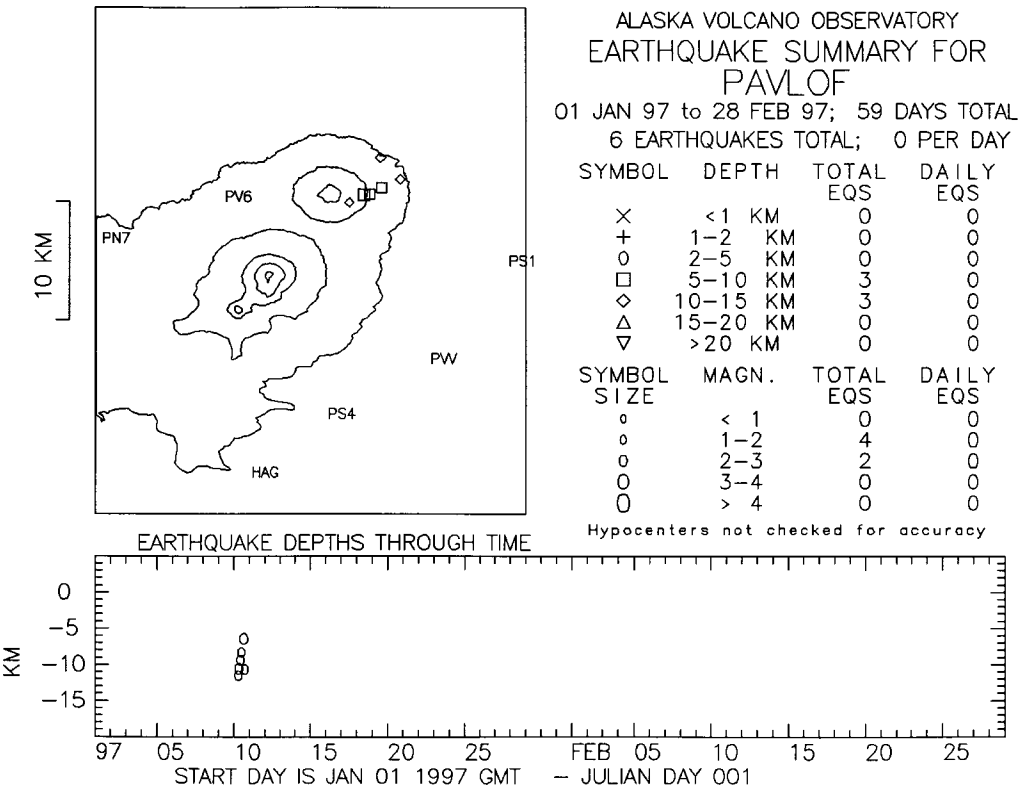

Figure 11a: Locatable Pavlof seismic events in space and time for January through February.

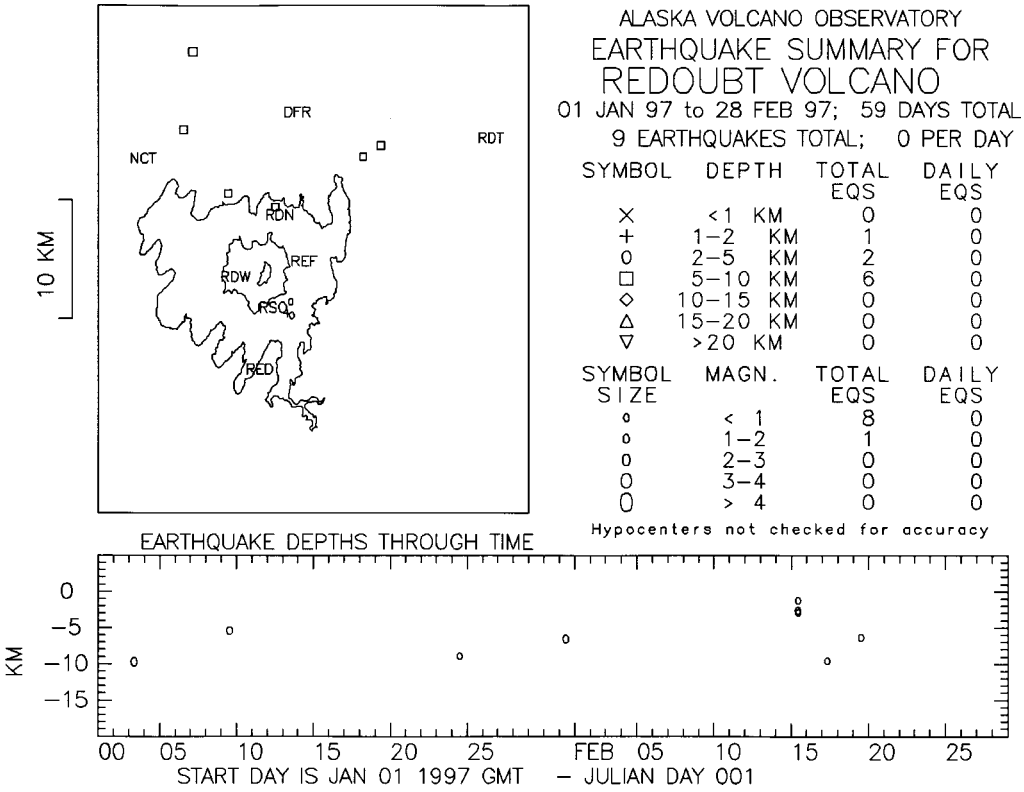

Figure 12a: Locatable Redoubt seismic events in space and time for January through February.

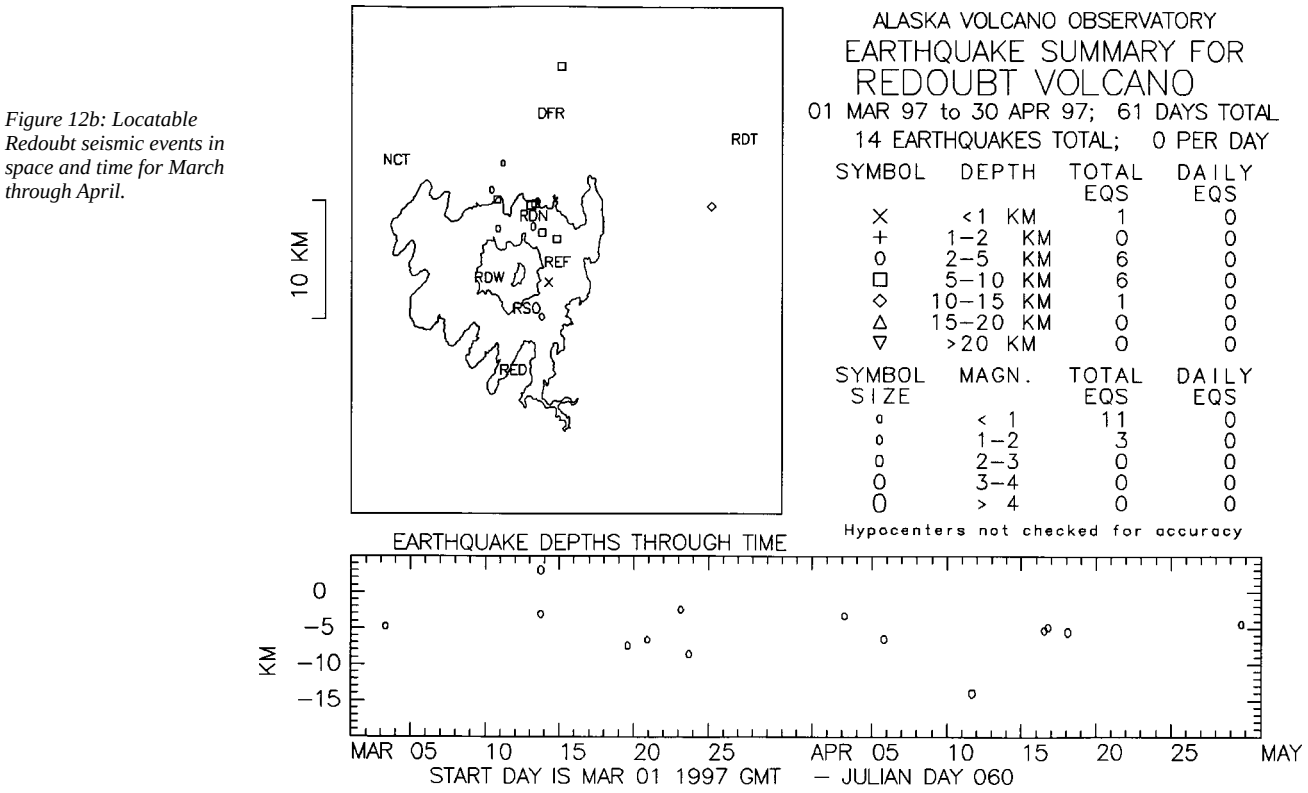

Figure 12b: Locatable Redoubt seismic events in space and time for March through April.

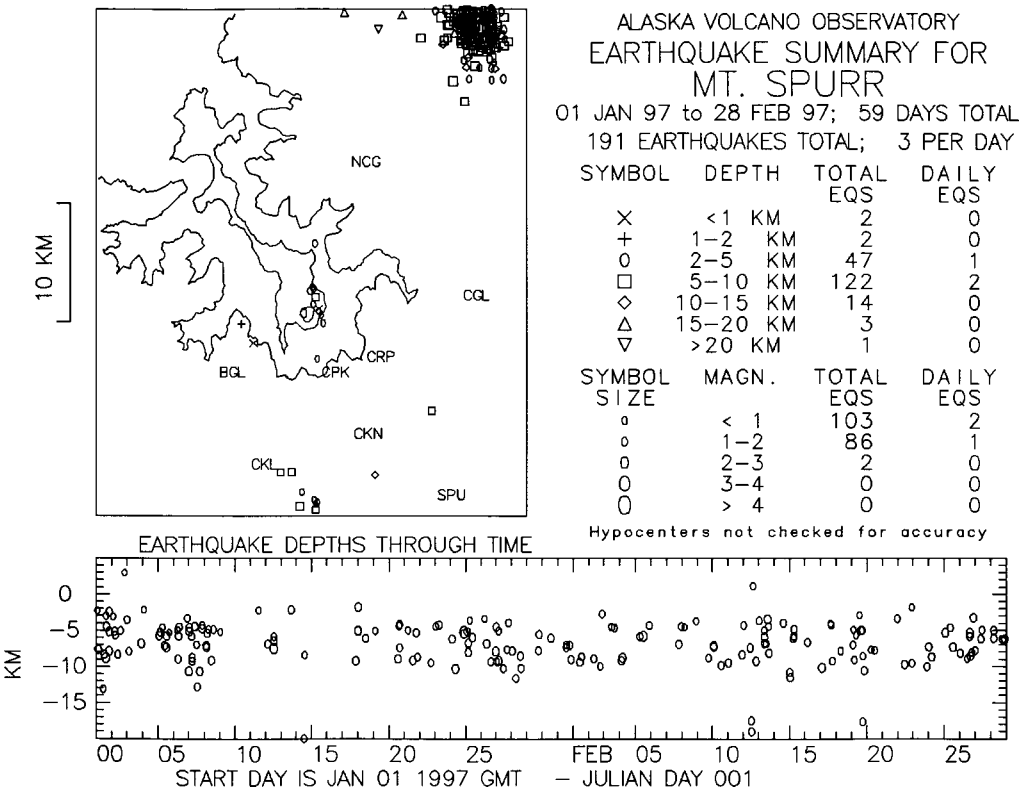

Figure 13a: Locatable Mt. Spurr seismic events in space and time for January through February. The cluster of events to the NE of Mt. Spurr is a tectonic swarm near Strandline Lake and is not related to the volcano.

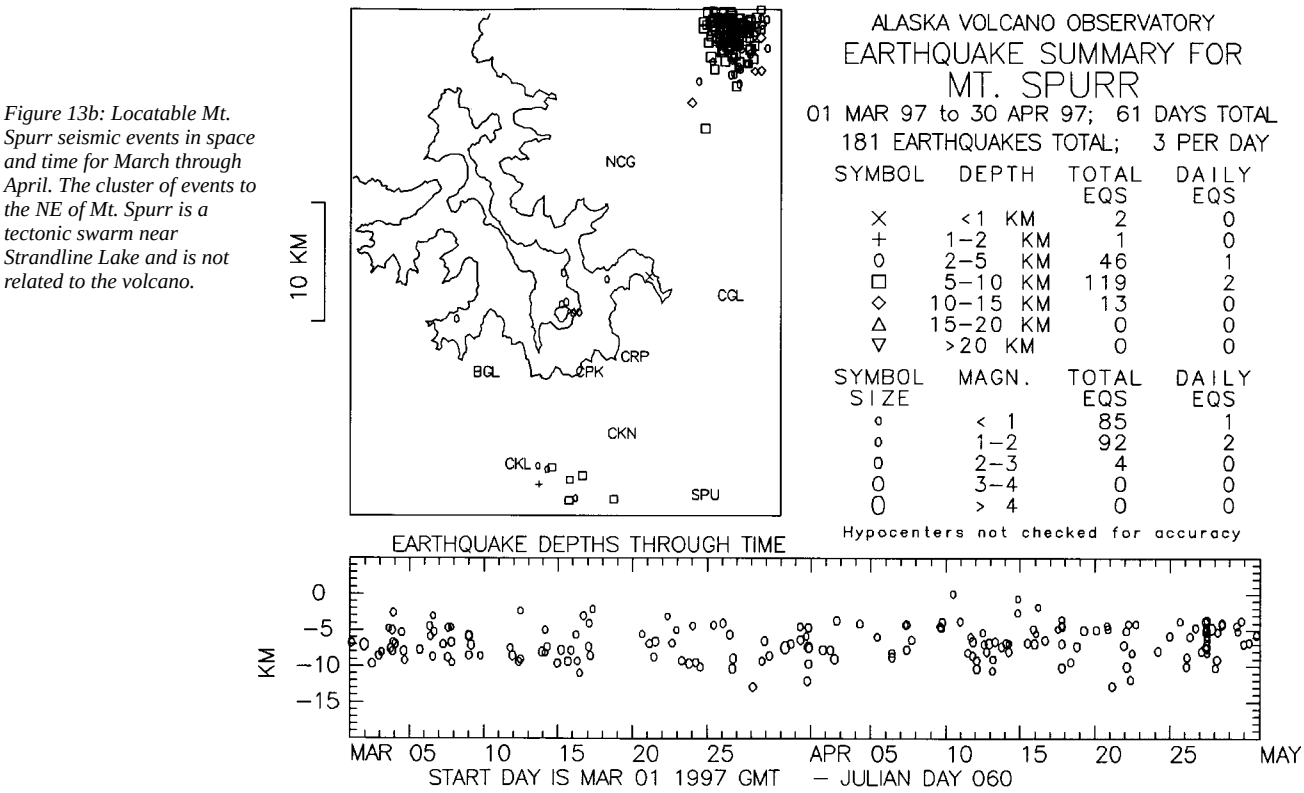

Figure 13b: Locatable Mt. Spurr seismic events in space and time for March through April. The cluster of events to the NE of Mt. Spurr is a tectonic swarm near Strandline Lake and is not related to the volcano.

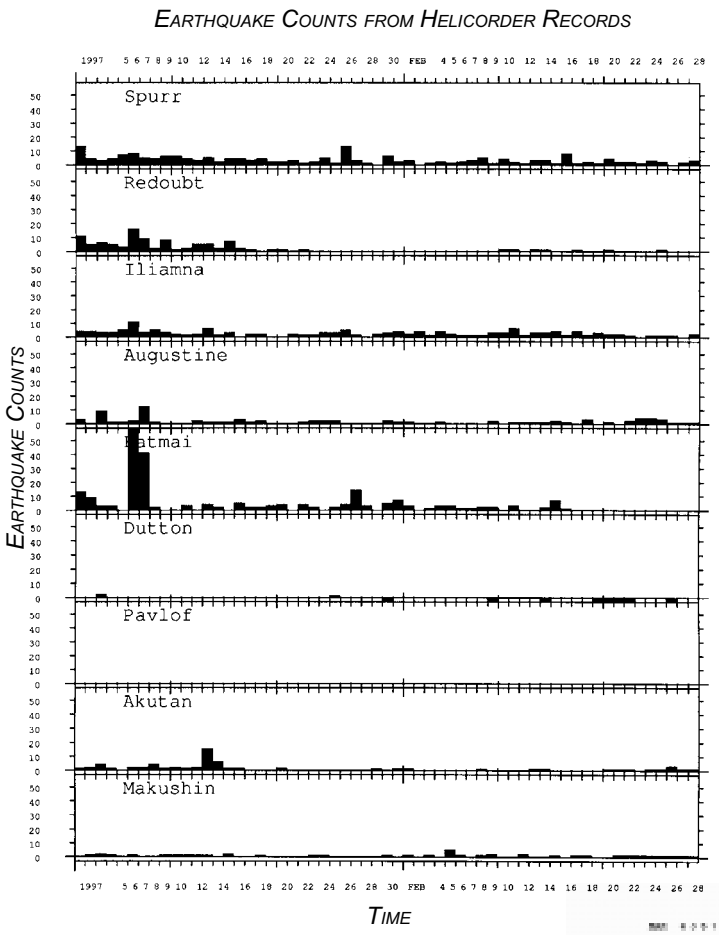

Figure 14a: Histogram of seismic events counted from helicorder records during January through February.

Figure 14b: Histogram of seismic events counted from helicorder records during March through April.

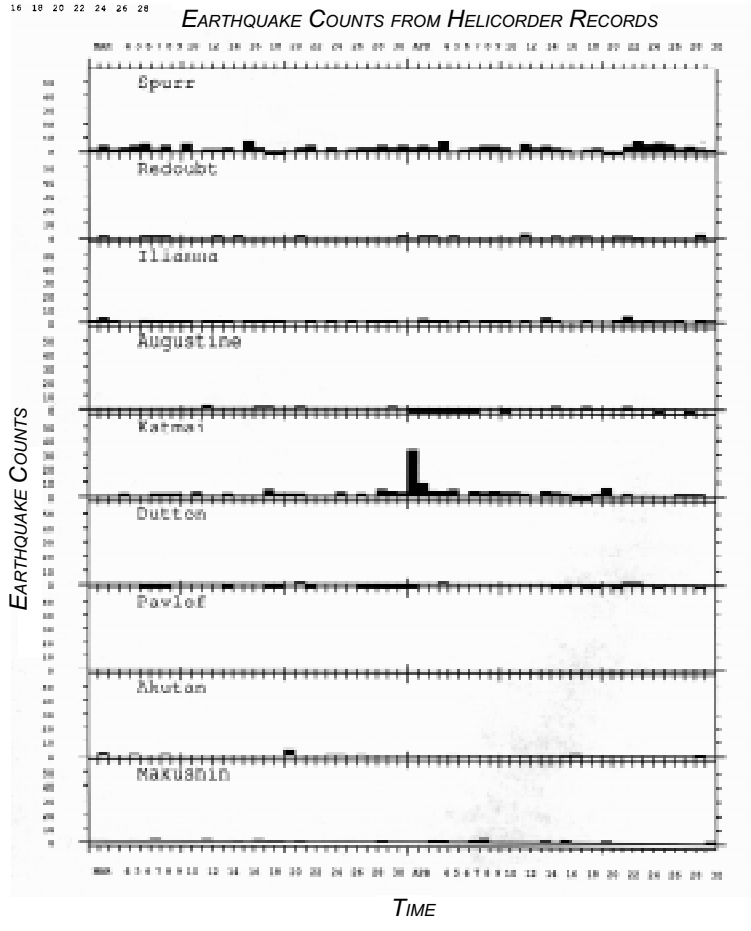

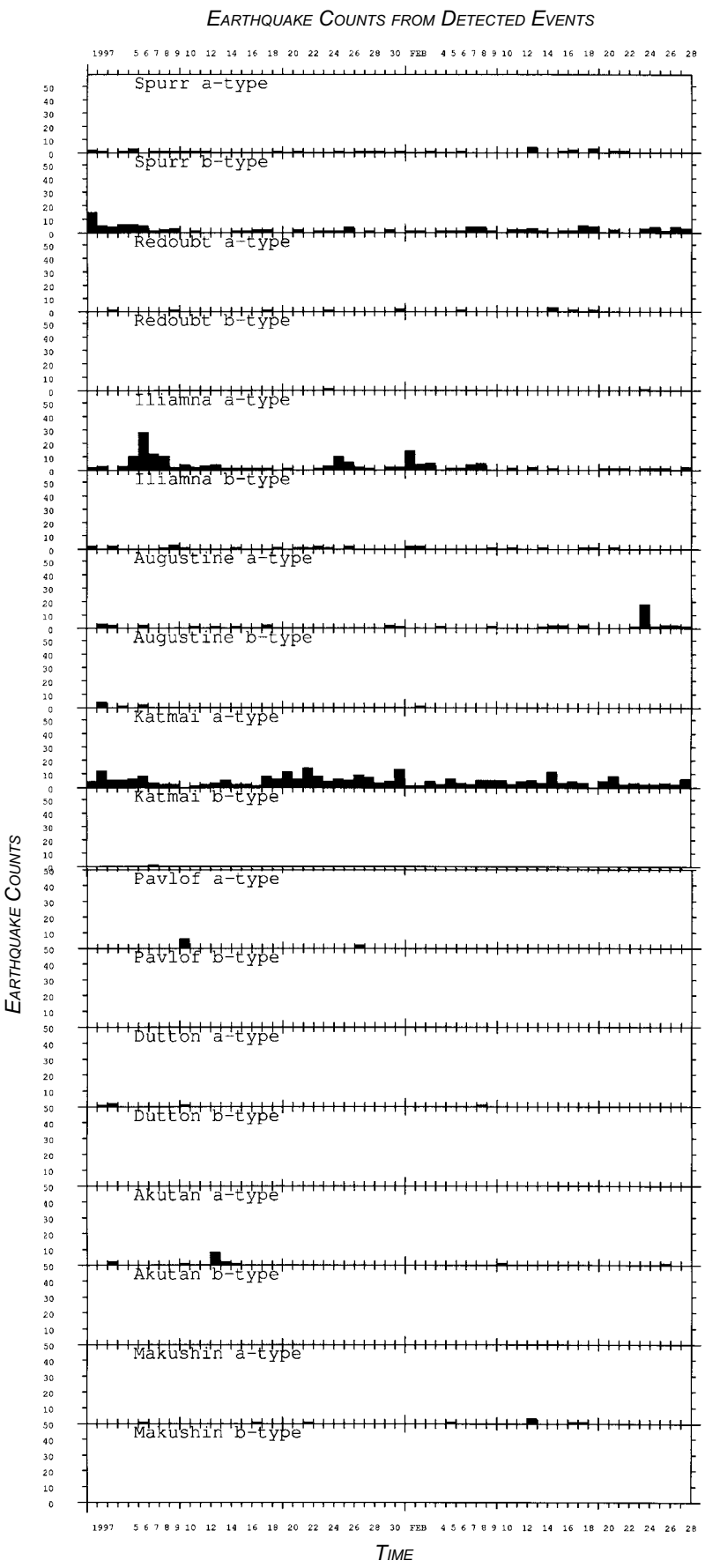

Figure 15a: Histogram of computer detected ("Willie system") seismic events during January through February.

Figure 15b: Histogram of computer detected ("Willie system") seismic events during March through April.

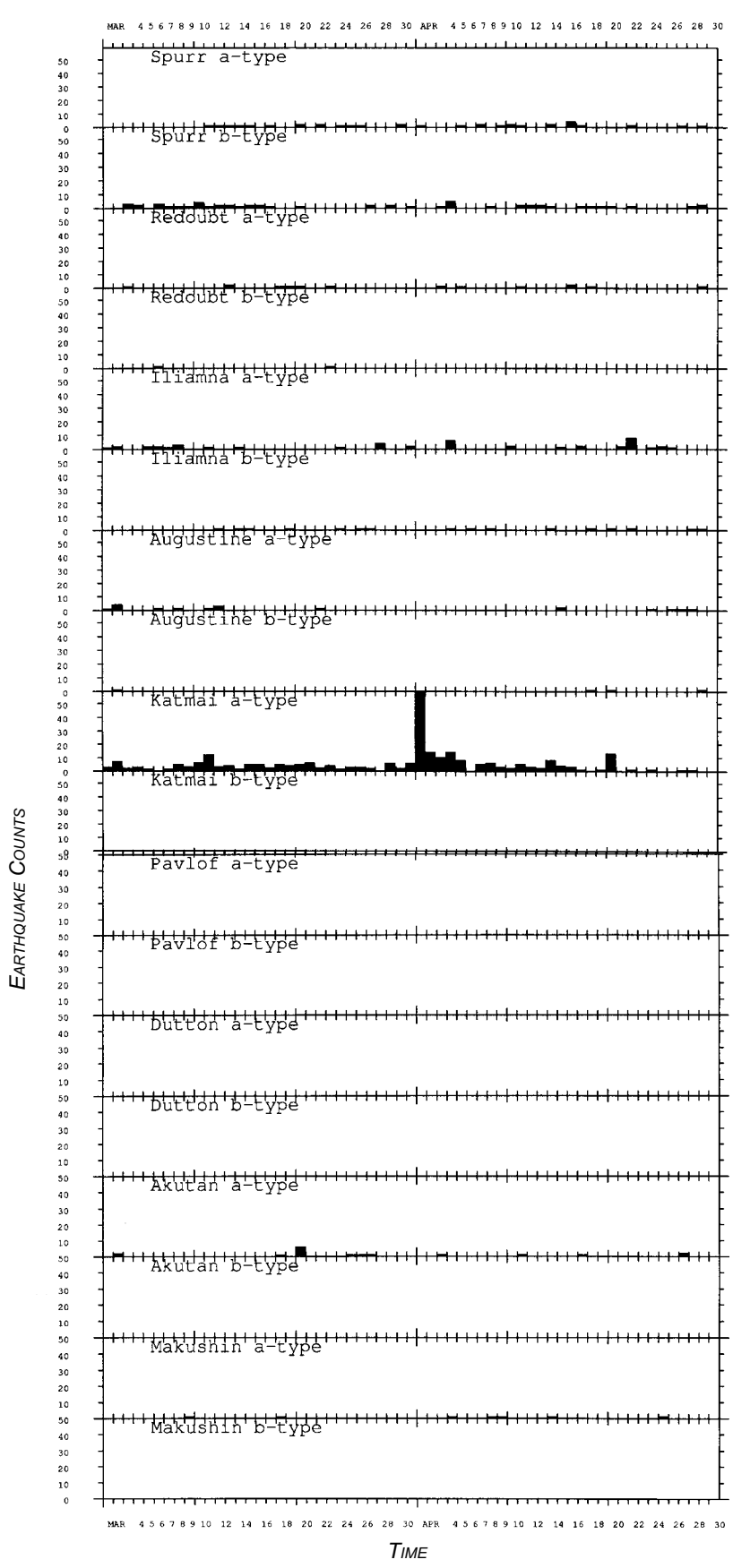

Observed Mean Seismicity Rates

The close of 1996 marked the accumulation of yet another year of seismic data. This seemed like a good time to use this additional data to revise the monthly earthquake averages of the various volcanoes monitored by AVO. For the time periods of 1994, 1995 and 1996, a total of 280 earthquakes were located in the Augustine area. However, not all these events appear to be actually related to activity at Augustine. If one does not include in the earthquake total those events believed to be of regional tectonic origin as well as those events suspected of being related to the interaction of shore-ice or in some other way related to cold weather, then the total number of earthquakes that appear to be actually related to Augustine activity would be 246 events. The three-year average seismicity rate for Augustine would, therefore, be 6.8 earthquakes per month.

For Redoubt, the three-year earthquake total is 364 located earthquakes with an average of 10.1 earthquakes per month. A total of 568 earthquakes were located in the vicinity of Spurr over this three-year period, which results in a mean value of 15.8 located events per month. Note that events of the Strandline Lake swarm have not been included in the calculation of this mean value.

As is apparent from almost any map of Spurr and Redoubt seismicity, a number of earthquakes plot quite some distance from these volcanoes and thus do not appear to be actually related to volcanic activity at these volcanoes. As a result, the mean seismicity rates given above for Redoubt and Spurr may be a bit misleading. If one only considers the seismicity within about a 10 km radius of the summits of Redoubt and Spurr, then the three-year earthquake totals for Redoubt and Spurr are 304 and 337 respectively. The resultant three-year average of the seismicity rate within the 10 km radii are 9.4 earthquakes per month for Spurr and 8.4 earthquakes per month for Redoubt. Note that the 10 km radius around the summit of Spurr includes the Crater Peak vent region. Part of the impetus for looking at seismicity within the 10 km radii is that the next generation of base maps for plotting the volcano seismicity are being prepared by Guy Tytgat. These maps will probably not cover exactly the same areas as those currently employed. Using the data from the 10 km radii should thus make future comparisons of seismicity rates a bit easier.

Determining the mean rate of seismicity at Iliamna is not nearly as straightforward as it was for the other three Cook Inlet volcanoes. During much of 1994 the Iliamna network was quite unreliable due to station outages. Such outages, for the most part, are due to the severe weather conditions (i.e. heavy snows combined with gale force winds) at Iliamna. Deep snow and unfavorable weather conditions prevented station maintenance at Iliamna until the September of 1994. Following this maintenance the Iliamna seismic network seems to have faired much better and has remained quite reliable. The incompleteness of the Iliamna data prior to September 1994 precludes its use in the mean seismicity rate calculation, however.

The level of seismicity at Iliamna during the May and August seismic swarms was far greater than had been previously observed there. This seismicity is quite significant and is not simply part of the day to day variation in the observed rate of seismicity. Inclusion of these data would very much skew the computed mean seismicity rate. Therefore, data from May and August-December should not be employed in any sort of seismicity rate estimates. The three years of data from which to determine the rate of seismicity at Iliamna has thus been reduced to a total of 22 months (1.8 years).

Calculating the mean seismicity rate for Iliamna is further complicated by the fact that an additional two stations (one of which has three-components) were deployed at Iliamna in late August,1996. This new station configuration resulted in a significant lowering in the seismic detection threshold at Iliamna. The justification for determining the mean rate of seismicity is to have some utility in defining background levels of seismicity for future reference and comparison. However, if data from the seismic swarms are excluded from the mean rate determination then the only data available are from the time period prior to the improvement of the Iliamna seismic network. Determining the mean rate of seismicity from these data would provide an estimate of the background level of seismicity prior to the installation of the new seismic stations. This mean value would not be valid for the more recent data in which the detection threshold has been considerably improved.

All is not lost, however. The data we do have can be used to generate a correction factor which when applied to the mean seismicity rate obtained from the original Iliamna network would predict the number of earthquakes that should be detected using the improved seismic network. Of course, there are all sorts of uncertainties involved with this method but lacking actual data it can at least give an estimate of what the background level of seismicity may be at Iliamna until sufficient data accumulate to actually perform a rate calculation. The data we have to work with are the detection threshold magnitude of the original Iliamna network, the mean rate of seismicity of that network, the detection threshold magnitude of the improved network, and an estimate of the present b-value. The standard magnitude-frequency of occurrence relation of Gutenberg and Richter (1941) is :

$$\log_{10}(N) = a + bM$$

where a and b are constants and N is the cumulative number of earthquakes greater than or equal to magnitude M. The value for b can be determined from the current Iliamna seismicity data and a is a constant for which some arbitrary value can be assumed. Substituting the detection threshold magnitude for M yields an estimate the cumulative number of earthquakes one would expect with that level of detection (and the assumed value of a). By doing this for both the detection threshold magnitude before and after the improvement of the network, one can get some idea of the relative difference in earthquake detection. The actual values of N are unimportant for our purposes; it is the ratio of the two numbers that is of interest. This ratio (i.e. $N_{new} : N_{old}$) is constant regardless of the value assumed for a and can be used to correct the seismicity rate data.

The correction factor, $N_{new} : N_{old}$, is the ratio of the estimated cumulative number of earthquakes obtained using the improved detection threshold magnitude to that obtained using the original detection threshold magnitude. The product of the mean seismicity rate from the original Iliamna network and this correction factor provides an estimate of what the mean number of earthquakes should be, given the improved detection capabilities of the present station configuration.

As noted above, the only data included in the mean seismicity rate computation for Iliamna are from the time period 09/94 - 04/96 plus data from 06/96 - 07/96. During this 22 month period, a total of 70 earth-

quakes were located at Iliamna. Therefore, the mean seismicity rate at Iliamna for this time period is 3.9 located earthquakes per month. The values of the detection threshold magnitudes and the present b-value estimate were obtained using the MATLAB® volcanic data script written by Stefan Wiemer. It turns out that the detection threshold magnitude of the original Iliamna network was 0.7, which is a bit higher than the 0.5 indicated in previous Bimonthly Reports. The present detection threshold magnitude at Iliamna was found to be 0.3. The b-value for the data from the time period after the network upgrade (08/28/97) until the writing of this article (07/16/97) is 1.23. Substituting these values into the Gutenberg and Richter equation, assuming some value for the constant *a* and taking the ratio of the two values of *N* results in a correction factor of 3.10. Multiplying the computed mean seismicity rate (i.e., 3.9 events/month) by this correction factor yields an estimated Iliamna seismicity rate with the improved network of 12.0 located earthquakes per month. Note that this calculation is assuming a perfect world in which all earthquakes having at least magnitude *M* are detected while those events smaller than this threshold go undetected. Both of these conditions are not totally valid. This estimate, however, is probably a pretty good first approximation.

One can also make preliminary estimates of the rate of seismicity of those volcanoes for which AVO has been monitoring for a relatively short period of time. Of course, in such a case the daily fluctuations in seismicity would have a much greater impact on the mean rate calculations than if such fluctuations were averaged out over a longer period of time. However, such a mean should at least provide an initial baseline for comparison until more data accumulate. The newly deployed seismic networks on Akutan, Makushin, Pavlof and Dutton were all in continuous operation as of August 1, 1996. Using this as the start date a six-month (i.e. 08/96 - 01/97) average seismicity rate was computed for these volcanoes. During this six-month period, a total of 69 earthquake were located in the Akutan region which results in a mean rate of 11.5 located events per month. Makushin had 17 located events or 2.8 events per month during this time period. A total of 12 earthquake were located near Pavlof which comes out to 2.0 located earthquakes per month. Because the current Dutton base map covers such a large area and Dutton is a fairly small volcano, only those events having locations within about a 5 km radius of the summit of Dutton were considered here. A total of 7 earthquakes were located within this radius which results in an average of 1.2 located earthquakes per month**.** Note, however, that these eleven events all occurred within a seven day a period. Therefore, they probably represent an anomalous seismic swarm rather than having any real bearing on the background level of seismicity. If this is the case, then a representative mean number of locateable earthquakes at Dutton would be considerably less than one event per month. With continued monitoring and the accumulation of additional data, this issue will eventually be resolved.

Determination of the mean rate of seismicity in the Katmai region is a bit more problematic than was the case with the other monitored volcanoes. AVO monitors at least six volcanic centers within the Katmai/Valley of Ten Thousand Smokes region. Therefore, seismicity plots for the Katmai region show a combination of seismic activity associated with each of the volcanic centers superimposed upon a background of regional tectonic seismicity. Ideally, one would like to estimate the mean seismicity rate of each of the volcanic centers within the Katmai region. However, doing so with the present plotting routine and basemap would be fairly involved. In the not too distant future, new plotting routines, databases and basemaps should allow one to determine the rate of seismicity associated with each of the volcanic centers quite easily. Until then a mean rate of seismicity for the entire region should at least provide a regional baseline for the area of Katmai and the Valley of Ten Thousand Smokes.

A difficulty results from the occurrence of a large swarm of seismicity in October. Over two-hundred earthquakes occurred in the Katmai/Valley of Ten Thousand Smokes region in a single day. Inclusion of these data would certainly skew the results of any sort of a mean seismicity rate calculation. Due to the uncertainties associated with defining the time of onset as well as that of the termination of this swarm, it is best to not include any data from October in the mean seismicity rate computation. Matters are further complicated by the fact that upgraded Katmai seismic network did not begin continuous operation until August 8, 1996. For the time period August, 1996 - January, 1997, there are a total of 19 weeks (4.75 months) of data for which a mean seismicity rate can be determined. During this time period a total of 616 earthquakes were located in the Katmai region. This comes out to be 32.4 events per week or 129.7 located earthquakes per month. Note that inclusion of the data from the October swarm results in a mean rate of seismicity rate 217.4 events per month, which illustrates just how greatly inclusion of such data can affect mean seismicity rate determinations.

The mean seismicity rates given in this article provide a baseline of the background levels of seismicity at each of the volcanoes. These values will be used for as a reference for the next year or until further notice. The mean rates of seismicity of the various volcanoes currently monitored by AVO are summarized in the table below.

Volcano	*Seismicity Rate Events/Month*	*Time Period of Average**
Augustine	6.8[A]	3-years
Redoubt	8.4/10.1[B]	3-years
Spurr	9.4/15.8[C]	3-years
Iliamna	12.0[D]	1.8 years
Akutan	11.5	6-months
Makushin	2.8	6 months
Pavlof	2.0	6 months
Dutton	1.2?[E]	6 months
Katmai	129.7	4.75 months

[A]This value does not include those events believed to be regional tectonic earthquakes and those events that appear to be related to shore-ice or are in some other way related to cold weather.

[B]The first value given is based upon only the seismicity located within a 10 km radius of the summit of Redoubt while the value to the right of the / included all of the data plotted on the current version of the Redoubt seismicity base map.

[C]The first value given is based upon only the seismicity located within a 10 km radius of the summit of Spurr while the value to the right of the / included all of the data, except for the Strandline Lake events, plotted on the current version of the Spurr seismicity base map.

[D]This is the predicted mean rate of seismicity for the present Iliamna seismic network. This value is not actually based upon seismicity located using this network. The above value is result of an attempt to computationally correct the mean seismicity rate from the original network to reflect the improved detection threshold of the present network. Note that due to station outages and two swarms of seismicity the entire three years of data were not included in that rate calculation (see text for more information).

[E]This value includes seismicity that may very well be a seismic swarm. If this is indeed the case then all one can really say is that the mean rate of seismicity at Dutton is much less than one located event per month.

**Data from the following time periods were used in the seismicity rate calculations for the given volcanoes - Augustine, Spurr and Redoubt: 01/94 - 12/96; Iliamna: 09/94 - 04/96, 06/96 - 07/96; Akutan, Makushin, Pavlof, and Dutton: 08/96 - 01/97; Katmai: 08/08/96 - 09/30/96, 11/96 - 01/97.*

Scott Stihler, Art Jolly, Chris Stephens, John Benoit, John Power, Bob Hammond, Steve McNutt, and Guy Tytgat

Augustine Deformation

The first third of 1997 has all three GPS receivers and co-located tiltmeters working well. We managed to collect GPS data throughout the winter with only a short downtime owing to a computer failure in Homer. The tiltmeters have not been so lucky. Although they are working, the data is suspect and not trusted. A field season is planned this summer to work on existing sites.

GPS

Figure 16 shows the GPS plots from MOUND-DOMO starting in April 1994. Most trends seem to have leveled out since the fall of 1996, about the same time westarted using the Ashtech SCA's at all sites. Figure 17 shows MOUND-WINDY data.

The data in 1997 appear to level off after a noisy fall in 1996.

TILTMETERS

Figure 18 shows the plots from DOMO tiltmeter. The radial tilt still is trending in the same direction with no apparent deviations. Figure 19 is the WINDY tiltmeter data and there is nothing unusual occurring at this site. Figure 20 is MOUND titlmeter data. The seasonal trend continues, with a bit more tilting on the x-axis this year.

Gene Iwatsubo

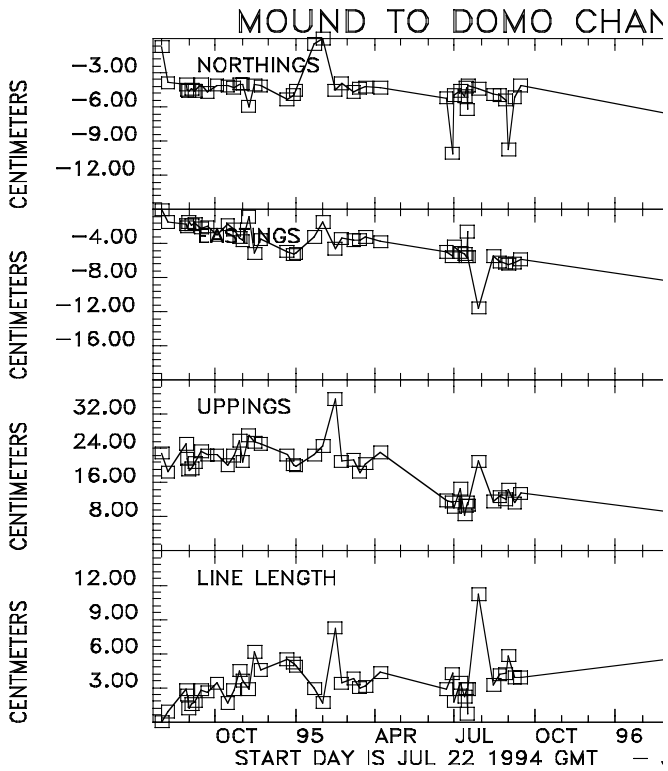

Figure 16a: Plots of the MOUND-DOMO GPS data starting in summer 1994. General trends in the data continue.

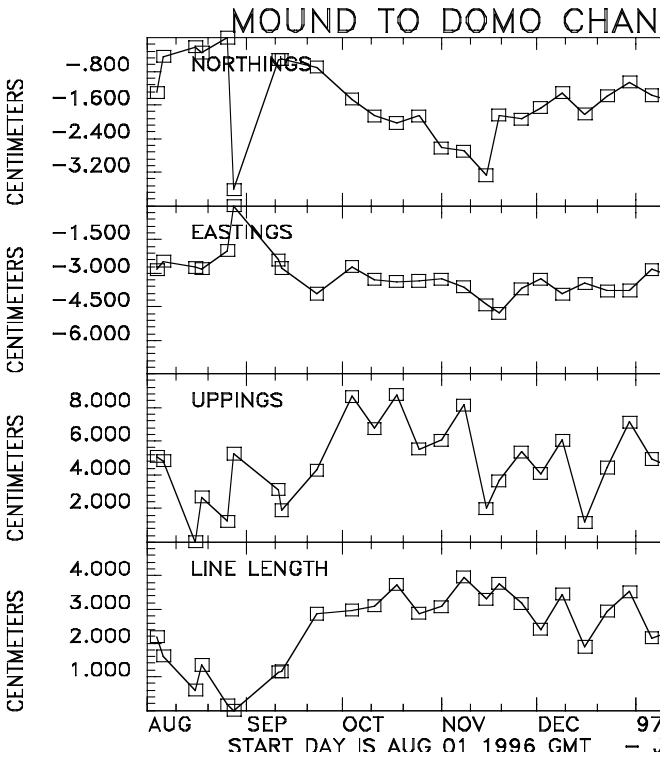

Figure 16b: Plots of the MOUND-DOMO GPS data starting in summer

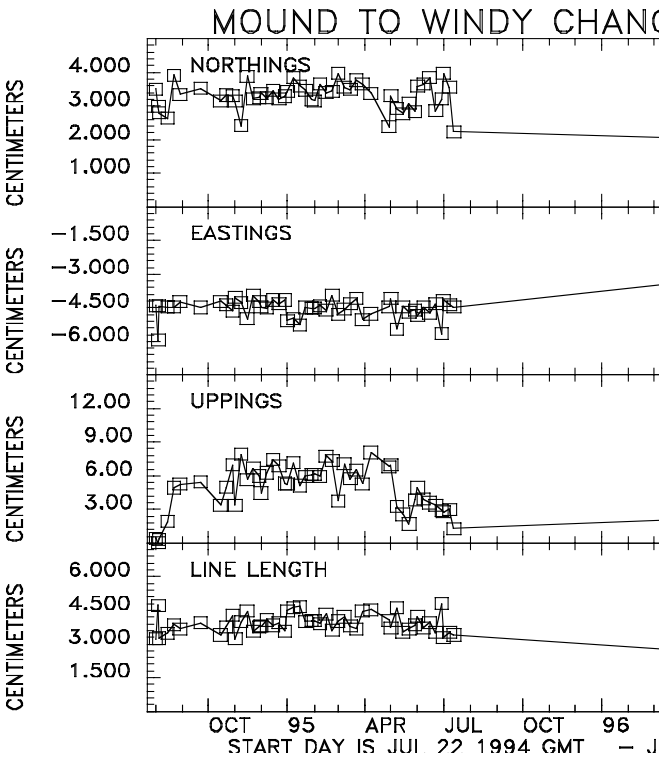

Figure 17a: Plots of the MOUND-WINDY GPS data starting in summer 1994. Data levels out in 1997.

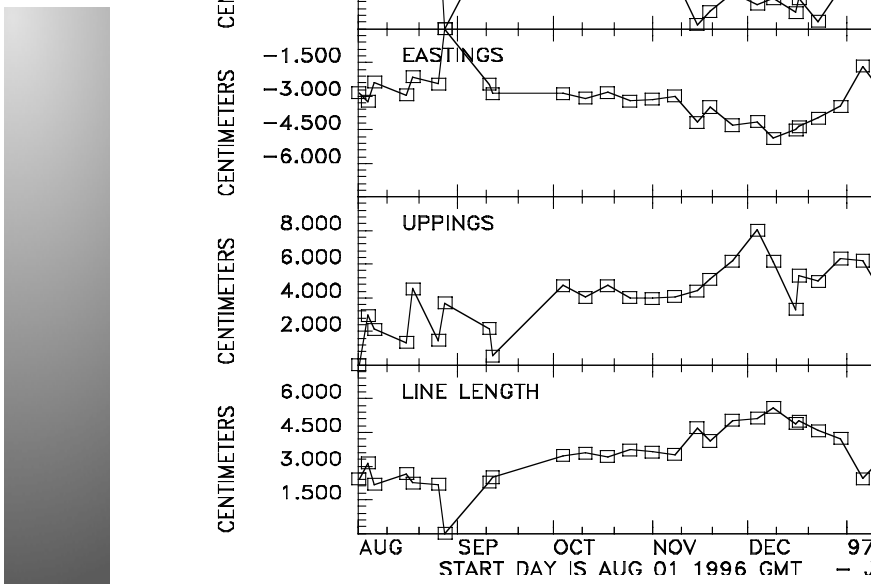

Figure 17b: Plots of the MOUND-DOMO GPS data starting in summer 1996.

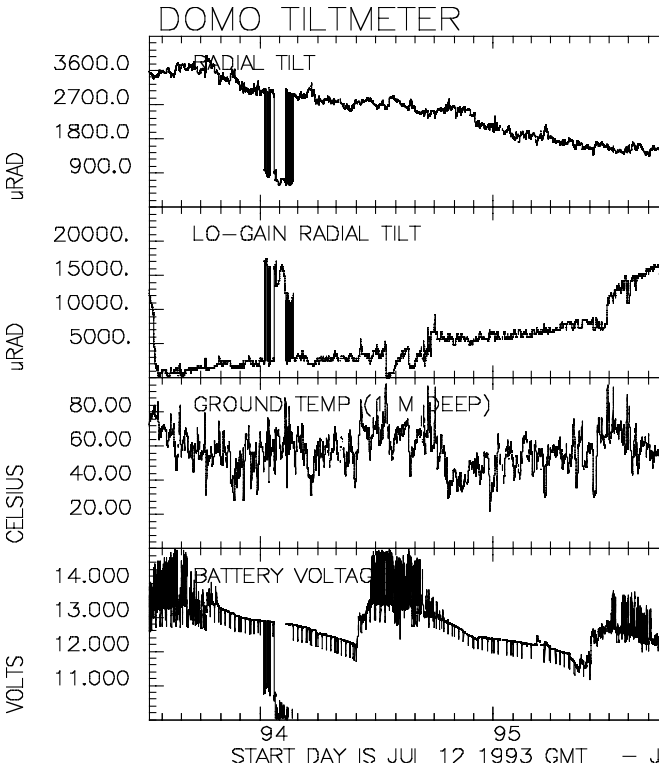

Figure 18: Plots of DOMO tiltmeter data. Major trends continue.

Figure 19: Plots of the WINDY tiltmeter data. Seasonal trends continue.

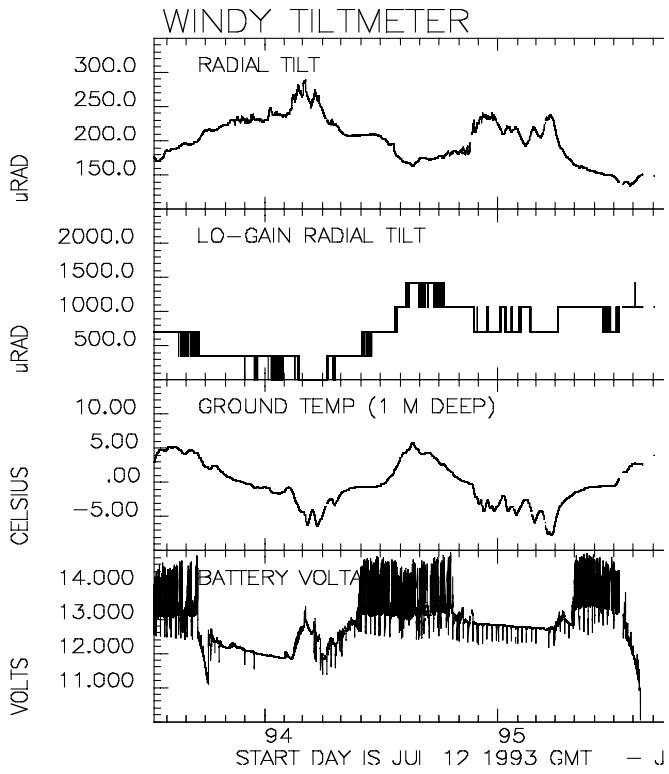

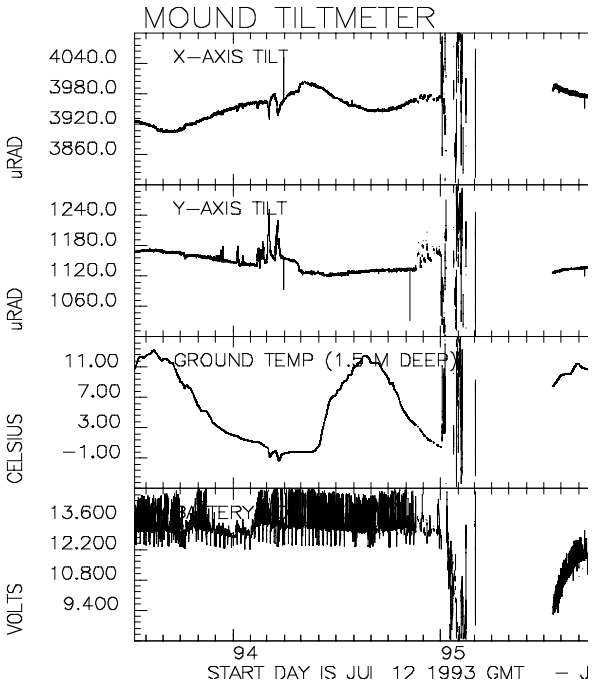

Figure 20: Plots of the MOUND tiltmeter data. Seasonal trends continue with a slight increase in April.

Operations

New Internal Web Site Permits Volcano Monitoring Via the Internet

During the winter and spring of 1997 AVO began building an internal web site for use primarily in volcano monitoring (fig 21). This page contains links to real-time or near-real-time seismic, satellite, and weather data. The site also contains an interactive log sheet of comments made by remote observers using the various data displays made availablefor the purposes of remote monitoring, and a calendar used for coordinating volcano watch duty within AVO.

It also contains phone lists and many other miscellaneous items handy for internal communication.The new web site displays seismological and satellite information that is processed enough to allow remote monitoring. Because the site is accessible over the Internet, monitoring can be done from anywhere - given a web browser and a telephone line. Thus, late-night, early-morning, and weekend volcano checks can be done from home by those with home computers. While this

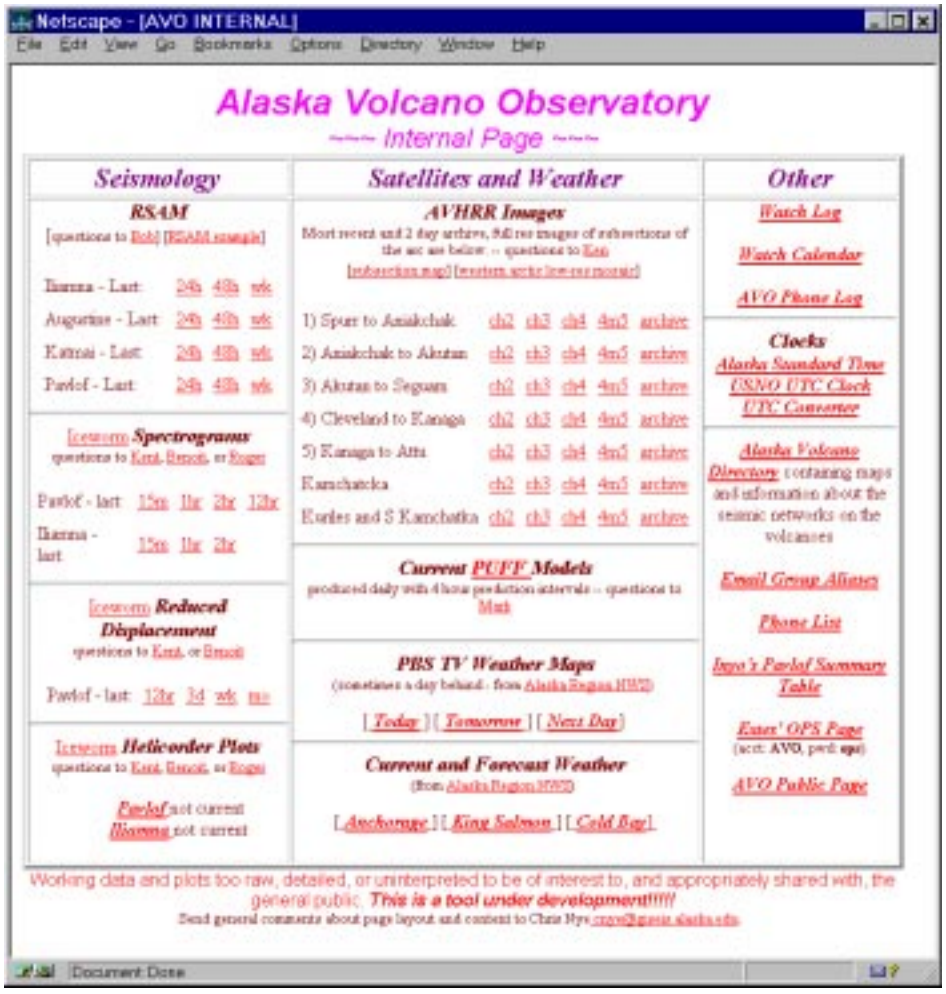

Figure 21: This is the HomePage of the AVO "intranet" which provides links to a variety of data displays and utilities located on the AVO web server and other computers.

system was under development there were periodic software crashes. An important point of the site is that there are multiple data displays and multiple data paths. Often when one crashed others didn't, so it was still possible to determine the state of the volcano. When watchers were unable to determine the state of the volcano they came into the lab to look at the Helicorder The new site does not permit detailed waveform analysis or location of earthquakes, and thus does not permit extended telecomputing.

RSAM

Real-time Seismic Amplitude Measurement (RSAM) computes and stores the average amplitude of ground shaking caused by earthquakes and volcanic tremor over 10-minute intervals. Increases in tremor amplitude or the rate of occurrence and size of earthquakes cause the RSAM values to increase. Rather than focusing on individual events, RSAM sums up the signals from all events during 10-minute intervals to provide a measure of the overall level of seismic activity. Figure 22 shows a sample RSAM plot. RSAM displays on the AVO internal web page cover the past 24 hours, past 48 hours, and past week. RSAM data plots are regenerated every 10 minutes and written to the webserver. Figure 22a shows RSAM data (right side) and seismograms (left side) form the eruptions of Mt. Redoubt on the 14th and 15th of December, 1989.

Spectrograms

The frequency content of seismic signals for several stations at each volcano are calculated in near real time and presented in a single panel for each volcano. Panels such as figure 23 present a sliding window of fifteen minutes of data from 5 stations. The plots are in color and updated every 5 to 10 minutes. The colors of the spectrogram represent the power of the seismic signal at a particular frequency. Warm colors represent high power. For each station the seismograms are plotted directly above the spectrograms for comparison. Smaller versions of the spectrograms are also created and pasted together to form 1-hr, 2-hr, and 12-hr mosaics (fig. 24). These mosaics permit longer-term tracking of the nature of seismicity, but can require long download times over slow modem connections.

The examination of the spectrogram allows a quick discrimination between signals generated by

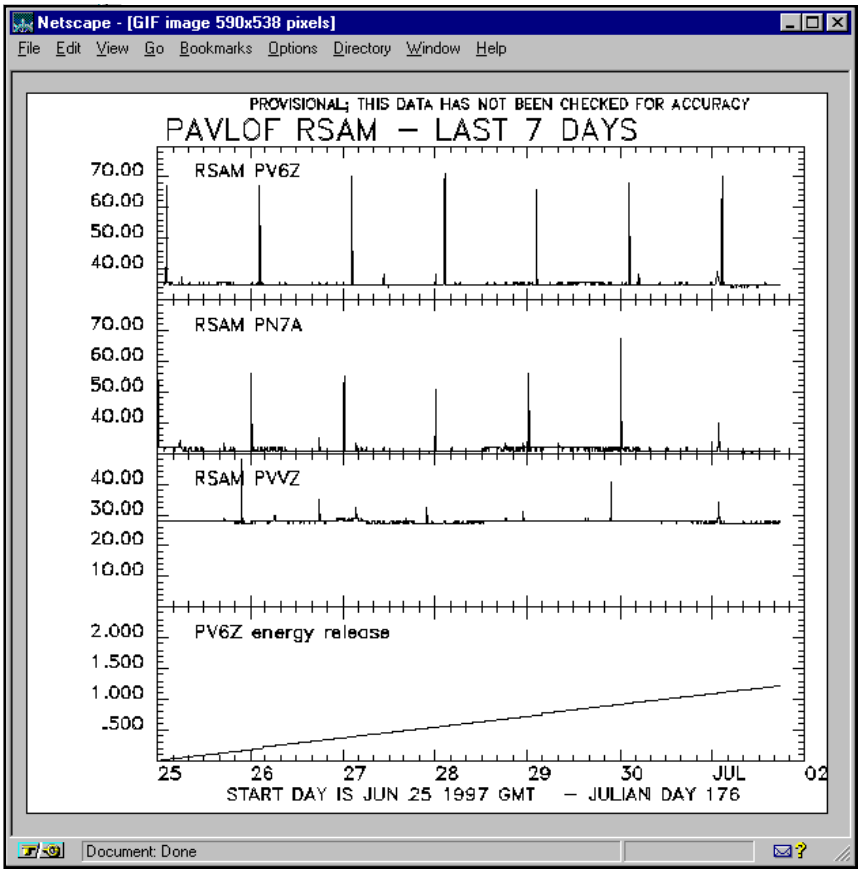

Figure 22: RSAM counts are generated by the PC-based Willie system and pasted to plots such as this. The large daily spikes are calibration pulses.

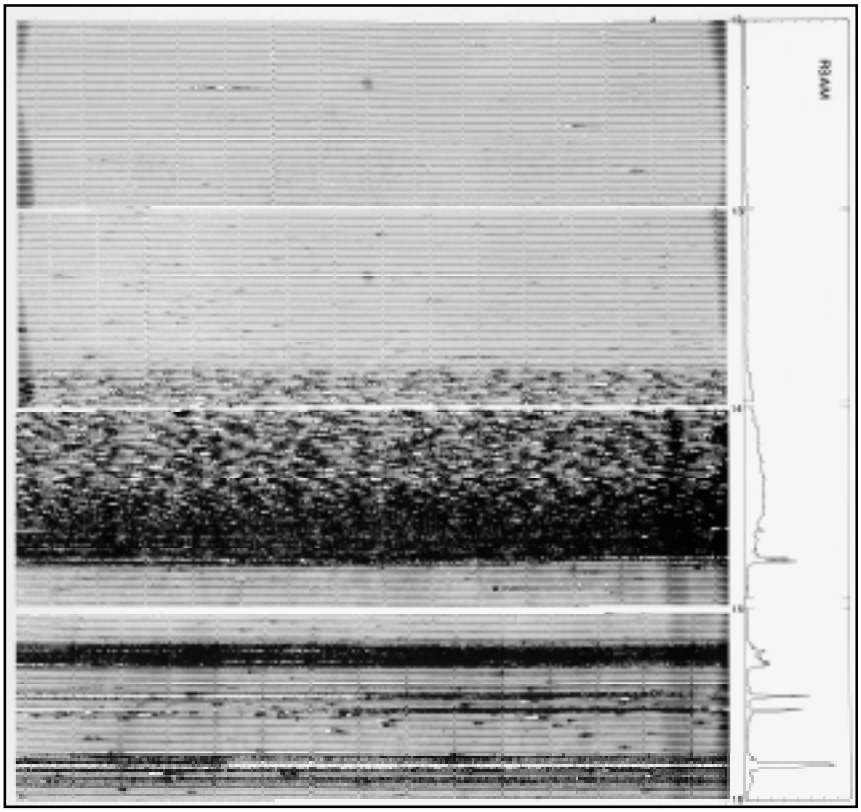

Figure 22a: RSAM example from Mt. Redoubt, 1989 (From RSAM webpage. example)

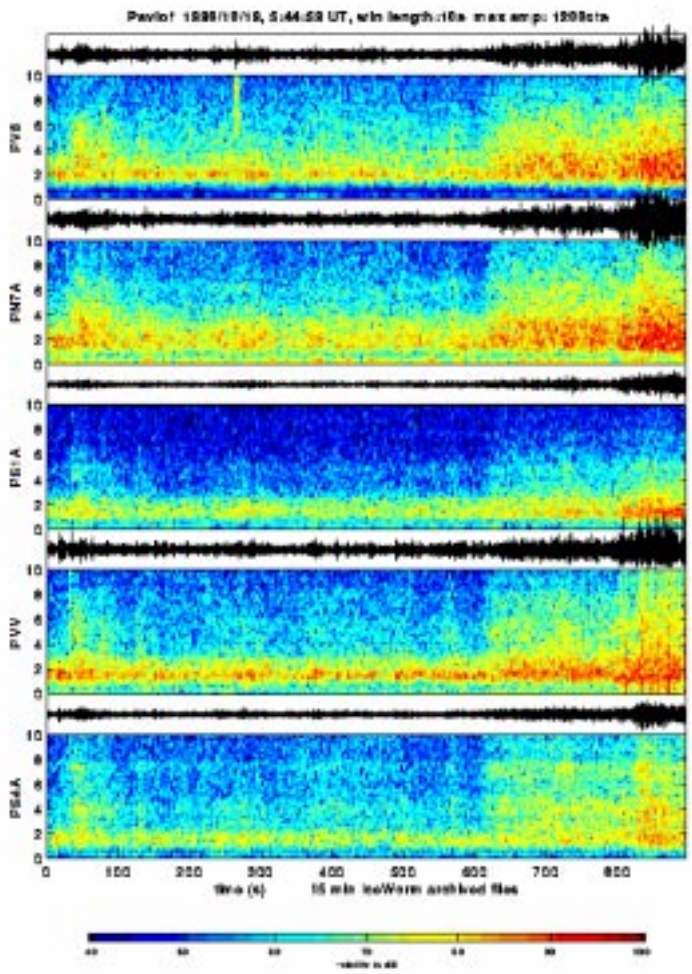

Figure 23: Fifteen minute spectra of five Pavlof stations. Data are from October 19, 1996 at the time code YELLOW was upgraded to code ORANGE. This plot clearly shows the 2hz low-level eruption tremor which becomes more broadband as the eruption intensifies.

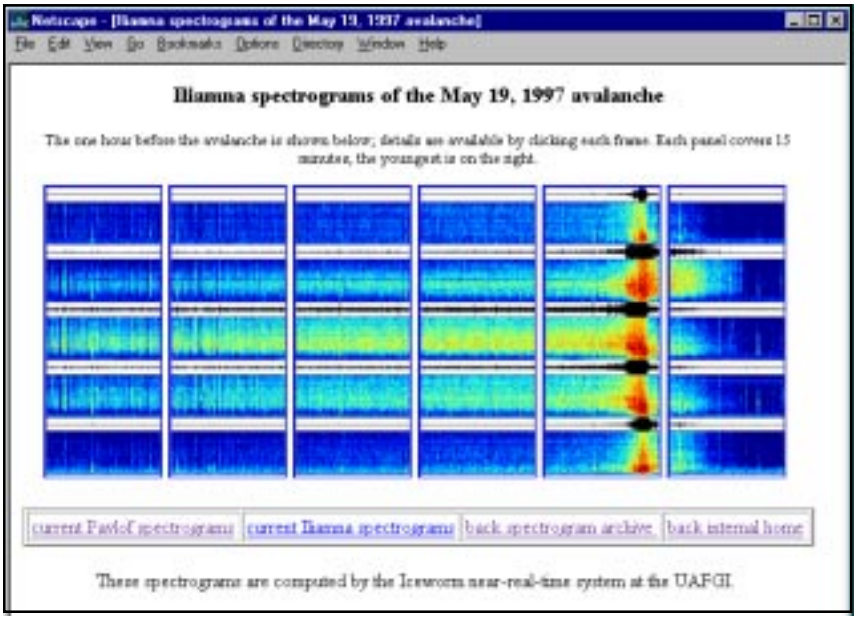

Figure 24: A one-hour mosaic of spectra showing the build-up to, and release of, the May 19, 1997 ice avalanche at Iliamna.

superficial and volcanic processes, such as the wind and tremor. Data are collected by ICEWORM, which is a UNIX-based automatic seismic data collection, and archiving system developed at the UAF/GI Seismology Laboratory and analyzed and plotted using ICEWORM and MATLAB. ICEWORM is an integration of USGS Earthworm, IRIS DATASCOPE, and custom UAF/GI/Seismology software.

Reduced Displacement

ICEWORM data are also used to calculate reduced displacement (a measure of seismic amplitude) in near-real-time. These are displayed on a single figure for each volcano (fig. 25) for a choice of periods ranging from 12 hours to a month. This makes it possible to track long-term changes is seismic intensity using reduced displacement, while spectrograms provide more detailed information about the short term nature of the seismicity. Reduced displacement data are also tied to automated paging and e-mail. An alarm is sent when the reduced displacement exceeds a preset threshold value. Surface wind speeds are also plotted so that storm-generated seismic amplitude increases can be easily recognized. Reduced displacement is similar to RSAM but has some significant differences. The seismic amplitudes are measured in the frequency domain, allowing non-volcanic signals such as storm-generated noise to be minimized. The reduced displacement measure also corrects for station-to vent distance and instrumental and recording system responses. This normalization allows for direct comparisons of many case histories and may constrain the size of the eruption. The amplitude of eruption tremor, as measured by the reduced displacement, has been shown to be directly related to the size of the eruption (McNutt 1994). Future systems may use the reduced displacement data to estimate starting plume heights for ash tracking programs such as PUFF. The reduced displacement and RSAM displays make use of independent computer systems, thereby increasing reliability.

Helicorder Plots

Pseudo-Helicorder plots (fig. 26) are generated in near-real-time using ICEWORM data and then posted on the web. These plots permit visual inspection of a day's worth of data at a single station on each figure. The pseudo-Helicorder plots provide advantages over the traditional drum records. The pseudo-Helicorder plots allow the signals to be filtered before being plotted. Filtering can significantly increase the signal-to-noise ratio and can reduce storm-generated noise. Also, these plots use no paper or valuable lab space. Currently, the disadvantages are that pseudo-Helicorder plots are created in near-

continued

real (up to 15 minute delay) time not real time, and that pseudo-Helicorder plots cannot be used for detailed waveform inspection because of llimitations of the GIF file format.

AVHRR Images

AVHRR data from NOAA weather satellites are received by the satellite ground station at UAF/GI. The data are processed specifically for monitoring volcanoes and detecting eruptions and other observable volcanic phenomena. Processing consists of subsectioning the images into six smaller images (fig. 27). This permits preserving the images at full resolution while maintaining a small enough file size that the images can be served over modem connections. Each image is geometrically and radiometrically corrected, and coastlines are added for reference. Finally, the images are translated to GIF files for internet use. For each subsection images of bands 2, 3, 4, and 4 minus 5 are prepared. The most recent image as well as a two day archive are available. Over 500 automatically processed images are generated each day. Presentation as GIF means that quantitative pixel temperatures cannot be directly obtained, as they can with the original Terascan images. Also common web browsers are not capable of color enhancement or enlargement, although the images can be downloaded to an additional software package. These images are sufficient for overview monitoring; details are extracted from the Terascan data. Anticipated improvements for the future include migrating to a file format that will permit determining pixel values

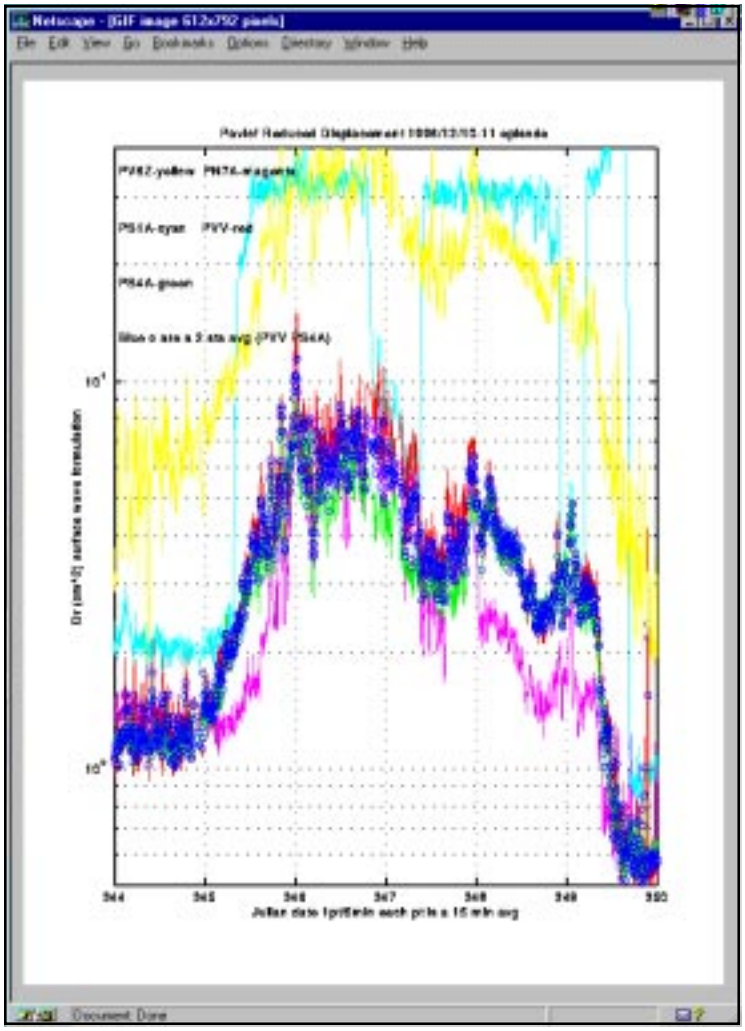

Figure 25: A six-day record of reduced displacement at Pavlof surrounding the December 10-11 eruptive pulse. The one day ramp-up to maximum eruptive intensity followed by a gradual 3-day decline can be readily seen. Each color represents an individual station. Circles are an average that is linked to the automatic alarm and paging system. Surface wind speeds are not

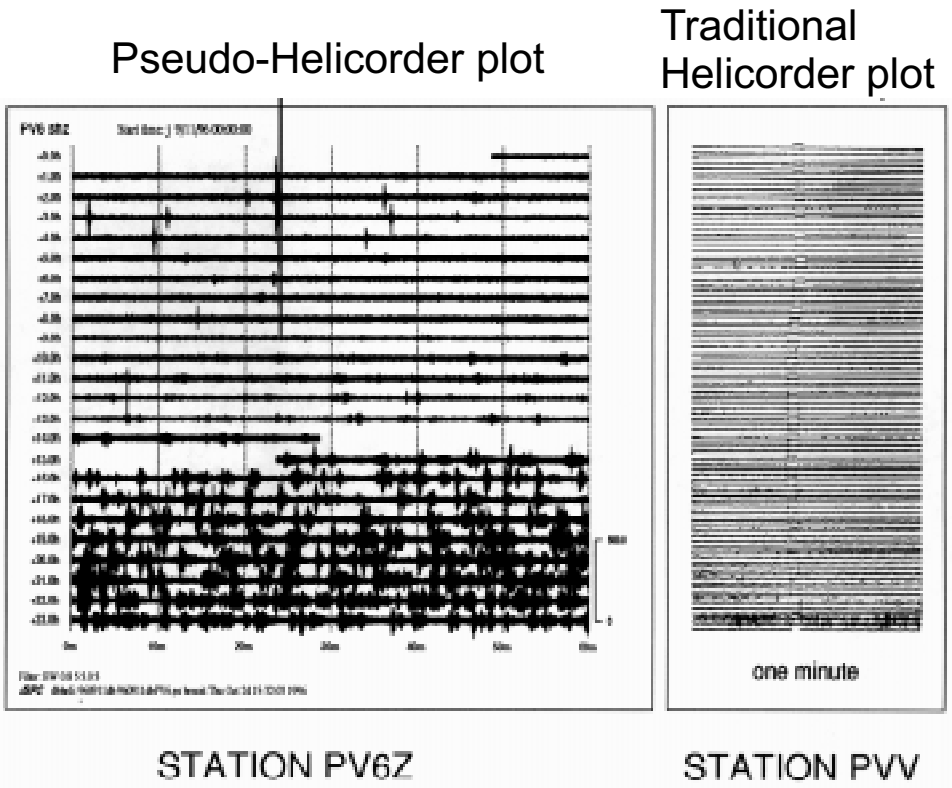

Figure 26: The PV6Z filtered pseudo-Helicorder plot and a one-minute section of the PVV helicorder record for September 11, 1996. The onset of a B-type earthquake swarm is clearly visible on the pseudo-Helicorder plot.

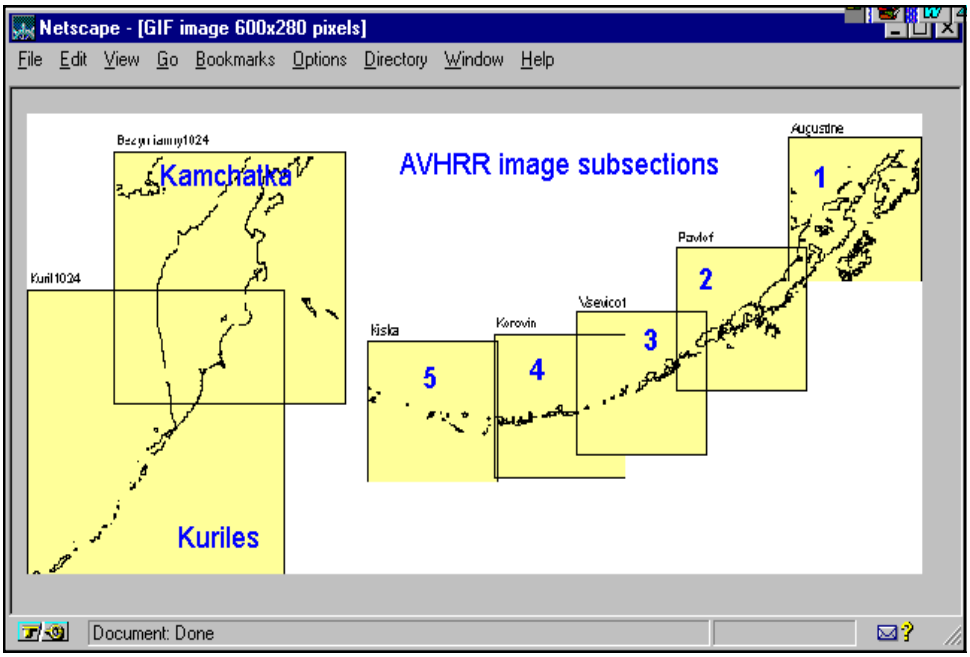

Figure 27: Sections that are cut out of full-resolution AVHRR images and used for volcano monitoring.

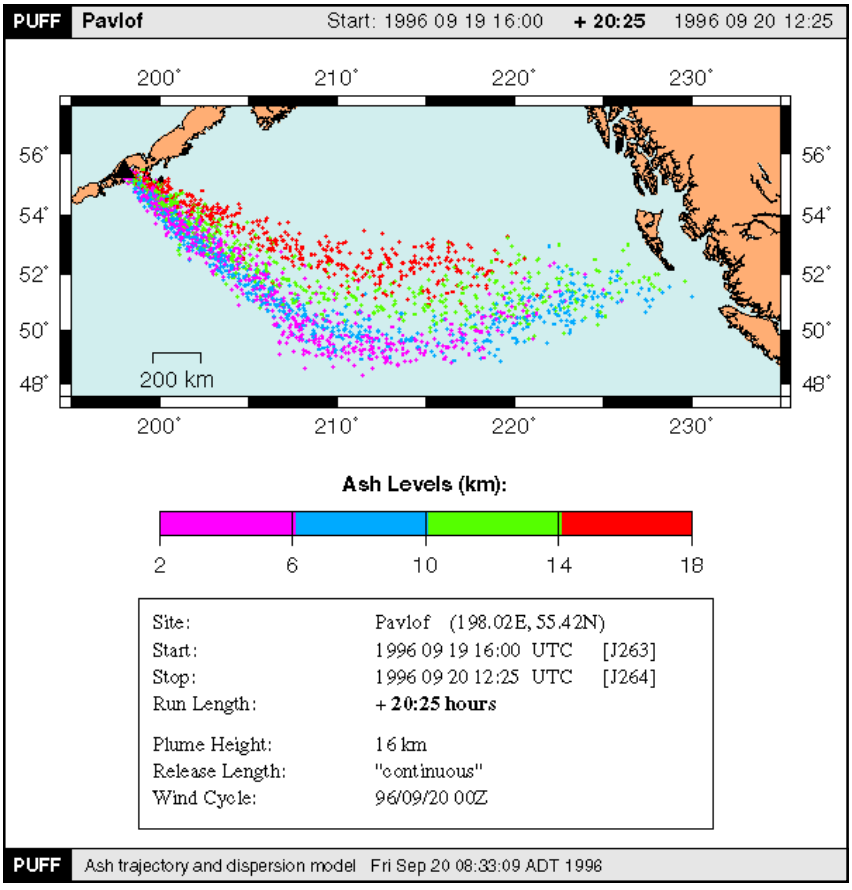

Figure 28: Example of current Puff model output.

over the web and automated detection and plotting of maximum pixel temperatures as a function of time.

PUFF Models

Puff is an ash trajectory projection model that tracks a hypothetical column of ash as it is dispersed down the wind field (fig. 28). Unidata windfield data are automatically obtained over the Internet, models are calculated for selected circum-Pacific volcanoes, and results in the form of GIF images are pasted to the web. The PUFF model was originally developed at UAF/GI and is in use at the GI and the NWS.

Watch Log and Watch Calendar

The AVO internal page also contains two interactive subpages used for logging information and scheduling observation times.

The Watch Log (fig. 29) is a perl script that observers use to interactively log information onto the AVO web server. The messages are compiled onto a single "bulletin board" and all messages are linked so previously posted messages can be "clicked on" and responded to, allowing multiple layers of discussion on various topics.

The Watch Calendar is an interactive calendar that observers use to sign up for volcano watch duty. This replaces the paper sign up sheet which hung by the Helicorders. It is useful in that it permits offsite observers to not only sign up for watches but also to view the most current schedule via the Internet. The Watch Calendar is also a perl script which was modified from a calendar script made freely available over the Internet.

continued

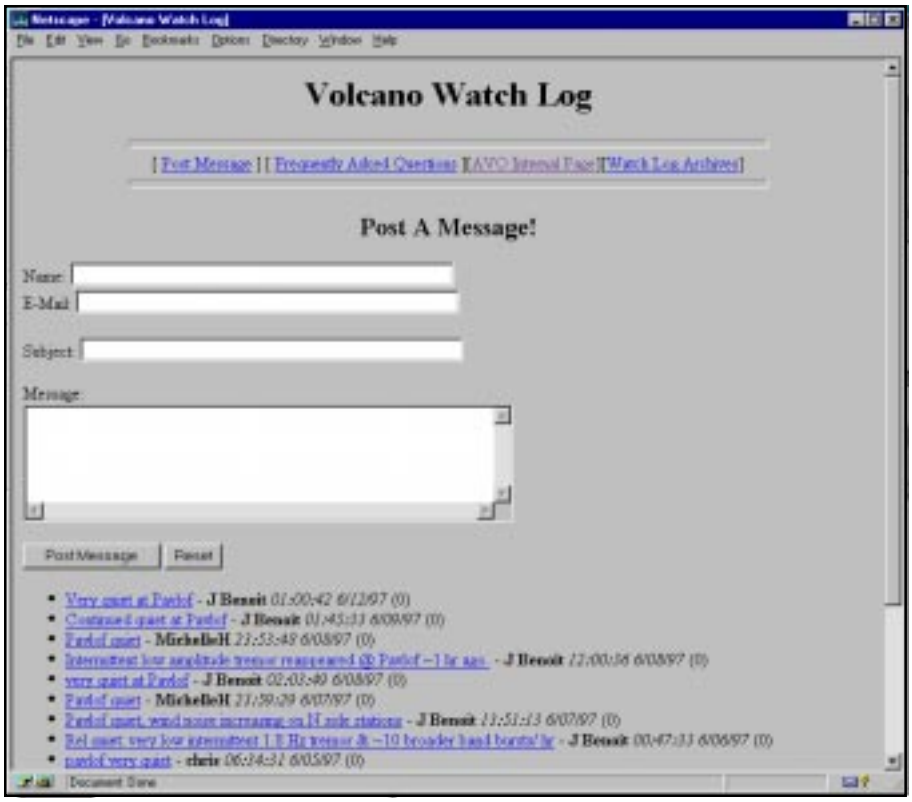

Figure 29: The entry form for the Watch Log, which provides an interactive way for remote users to log on via the internet and discuss observations.

Figure 29a: The Watchlog Calendar

System Resources

The Iceworm seismic data and collection and processing system runs on a Sun 200 Mhz Ultra 2 workstation, which handles over 200 seismic stations for both volcano and regional earthquake monitoring. A complete backup system runs on a dual-processor SPARC-20 workstation. The web site is served by a dual-processor 150 Mhz SPARC-20 workstation.

Chris Nye, John Benoit, Bob Hammond, Kevin Engle, Katherine Queen, Kent Lingquist, Mark Servilla, and Ken Dean

Reference:
McNutt, S.R., Volcanic tremor amplitude correlated with eruption explosity and its potential use in determining as hazards to aviation, USGS Bull 2047, p. 377-886, 1994.

Makushin Geologic Map

During the early months of 1997, I began the work of compiling field and geochemical data to create the geologic map for the Makushin Volcanic Field. Kathy Queen of ADGGS has the daunting task of creating the ArcInfo document. The completed document will be published as a ADGGS Professional Report. There will be two sheets, one with the geologic map, map unit descriptions, cross-section, and a geologic discussion. The second sheet will contain a sample location map, whole rock/trace element data, $^{40}Ar/^{39}Ar$ age determination data, ^{14}C age data, and several figures. Our aim with this publication is to highlight the eruptive history of this volcanic field creating a template for determining risk factors from future eruptions. The map will contain both bedrock and Quaternary volcanic deposits. My co-authors, C. Nye, J. Beget, A. Roach, K. Bean have been generous with their support and feedback and I thank them for their time and effort. Although the map was scheduled to go into review for ADGGS publication in late April, I have delayed this date in order to complete the $^{40}Ar/^{39}Ar$ data reduction.

V.S. McConnell